BMC Biology

RESEARCH ARTICLE

Open Access

Imprinted *Grb10*, encoding growth factor receptor bound protein 10, regulates fetal growth independently of the insulin-like growth factor type 1 receptor (*Igf1r*) and insulin receptor (*Insr*) genes

Kim Moorwood[1], Florentia M. Smith[1], Alastair S. Garfield[1] and Andrew Ward[1*]

Abstract

Background Optimal size at birth dictates perinatal survival and long-term risk of developing common disorders such as obesity, type 2 diabetes and cardiovascular disease. The imprinted *Grb10* gene encodes a signalling adaptor protein capable of inhibiting receptor tyrosine kinases, including the insulin receptor (Insr) and insulin-like growth factor type 1 receptor (Igf1r). *Grb10* restricts fetal growth such that *Grb10* knockout (KO) mice are at birth some 25-35% larger than wild type. Using a mouse genetic approach, we test the widely held assumption that Grb10 influences growth through interaction with Igf1r, which has a highly conserved growth promoting role.

Results Should Grb10 interact with Igf1r to regulate growth *Grb10*:*Igf1r* double mutant mice should be indistinguishable from *Igf1r* KO single mutants, which are around half normal size at birth. Instead, *Grb10*:*Igf1r* double mutants were intermediate in size between *Grb10* KO and *Igf1r* KO single mutants, indicating additive effects of the two signalling proteins having opposite actions in separate pathways. Some organs examined followed a similar pattern, though *Grb10* KO neonates exhibited sparing of the brain and kidneys, whereas the influence of *Igf1r* extended to all organs. An interaction between Grb10 and Insr was similarly investigated. While there was no general evidence for a major interaction for fetal growth regulation, the liver was an exception. The liver in *Grb10* KO mutants was disproportionately overgrown with evidence of excess lipid storage in hepatocytes, whereas *Grb10*:*Insr* double mutants were indistinguishable from *Insr* single mutants or wild types.

Conclusions Grb10 acts largely independently of Igf1r or Insr to control fetal growth and has a more variable influence on individual organs. Only the disproportionate overgrowth and excess lipid storage seen in the *Grb10* KO neonatal liver can be explained through an interaction between Grb10 and the Insr. Our findings are important for understanding how positive and negative influences on fetal growth dictate size and tissue proportions at birth.

Keywords Cell signalling, Developmental biology, Epistasis, Fetal growth, Genomic imprinting, Insulin, Steatosis, Insulin-like growth factor, Mouse genetics

*Correspondence:
Andrew Ward
bssaw@bath.ac.uk
[1] Department of Life Sciences, University of Bath, Building 4 South, Claverton Down, Bath BA2 7AY, United Kingdom

Background

Mammalian fetal growth is a highly regulated process influenced positively and negatively by genetic and environmental factors, including maternal nutrient supply. Attaining an appropriate size is strongly correlated with infant survival [1] and minimises the risk in later life of common disorders including obesity, diabetes and cardiovascular disease (see [2, 3]). The insulin/insulin-like growth factor (Ins/IGF) signalling pathway is conserved, most likely throughout animal species, to regulate growth and energy homeostasis, as well as being a major determinant of longevity [4, 5]. Involvement of the target of rapamycin complex (TOR or mTOR in mammals) is similarly broadly conserved, linking nutrient sensing, growth factor signalling and protein translation control with the same processes [5]. The invertebrate pathway involves a single Ins/Igf receptor that mediates all of these functions. In mammals the regulation of energy metabolism is a separate function of insulin acting through the insulin receptor (Insr), while the structurally related Igf1r is the primary mediator of fetal growth (Fig. 1A). This was established through a series of elegant mouse genetic experiments that also linked fetal growth regulation with genomic imprinting [6]. These experiments proved that Igf1 and Igf2 stimulate fetal growth through the Igf1r, while a second, structurally unrelated receptor, Igf2r, inhibits growth by acting as a sink for Igf2. Further, they revealed that both *Igf2* and *Igf2r* are regulated by genomic imprinting, a form of epigenetic gene regulation that restricts expression to only one of the two parental alleles. The mouse genome contains around 150 imprinted genes, with just over half expressed predominantly from the paternally inherited allele and the rest expressed from the maternally inherited allele [7, 8]. Imprinted genes are diverse in their functions and the products they encode, but notable among them are genes encoding signaling proteins that regulate growth of the fetus, placenta, or both. These genes tend to fit with the most widely accepted hypothesis for the evolution of genomic imprinting in mammals, which posits a conflict between parental alleles in offspring that can influence nutrient acquisition from the mother [9, 10]. Noting that a female may have multiple mates, it is in the father's interest to maximise fitness of his offspring in an opportunistic manner, whereas the mother favours a more even distribution of resources to offspring throughout her reproductive span. These pressures have resulted in the expression in developing offspring of growth-promoting genes from paternally inherited alleles, such as *Igf2* and *Dlk1*, and growth restricting genes from maternally inherited alleles, such as *Cdkn1c*, *Grb10*, *Igf2r* and *Phlda2* [11, 12].

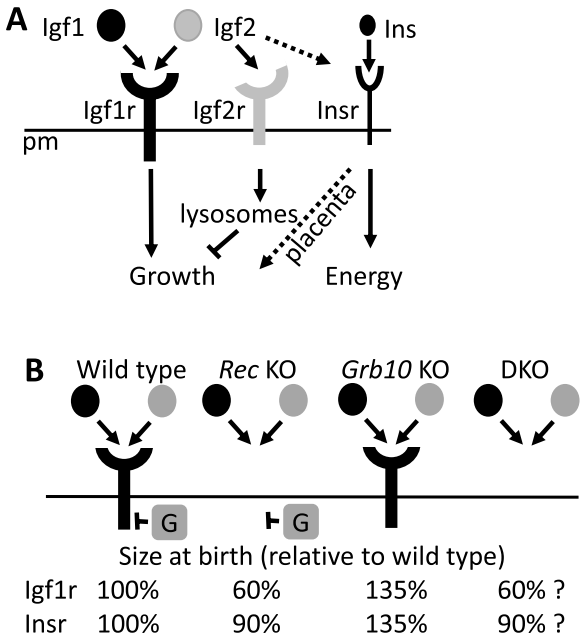

Fig. 1 Signalling interactions within the insulin/insulin-like growth factor pathway inferred from biochemical and mouse genetic studies. **A** The Igf1 and Igf2 ligands bind and activate Igf1r to promote fetal growth, whereas insulin (Ins) activates the Insr predominantly to regulate energy homeostasis (solid arrows). In the placenta, Igf2 also binds Insr, though with lower affinity than it does the structurally related Igf1r, to promote fetal growth (shown by the dashed arrows). Igf2 is also bound by Igf2r and thereby targeted for lysosomal degradation, such that Igf2r has an inhibitory action on fetal growth through sequestration of Igf2. Products of imprinted genes, paternally expressed *Igf2* and maternally expressed *Igf2r*, are shaded (grey). **B** Fetal growth outcomes expressed as mass at birth in mice of genotypes relevant to this study. Knockouts of either the *Igf1r* or *Insr* (*Rec* KO) previously shown to be growth restricted to 60% [41] and 90% [43] the size of wild type animals, respectively, while *Grb10* KO pups are enlarged at 135% [24–26]. If Grb10 should act predominantly on either receptor to inhibit growth then double knockout (DKO) mice, generated in the present study, should be indistinguishable from the respective receptor single KO pups

The importance of IGF signalling and imprinting for human fetal development is exemplified by characteristic overgrowth in Beckwith-Wiedemann syndrome (BWS), associated with excess *IGF2* expression, and growth restriction in Silver-Russell syndrome (SRS) associated with loss of *IGF2* expression [11–13].

Growth factor receptor-bound protein 10 (Grb10) is a signaling adaptor protein, capable of interacting with numerous different receptor tyrosine kinases (RTKs), typically inhibiting receptor activity and downstream signalling (reviewed in [14–16]), in at least some cases through a mechanism involving phosphorylation of Grb10 by the mTORC1 complex [17–21]. *Grb10* is unusual among imprinted genes in being expressed predominantly from

the paternal allele in the developing and adult central nervous system (CNS), and from the maternal allele in tissues outside of the CNS [22–24]. Mice with a germline knockout of the maternal *Grb10* allele ($Grb10^{m/+}$) are at birth around 30% larger by weight than wild type littermates [24–26], establishing a role for maternal *Grb10* as a potent inhibitor of fetal growth. While the mass of organs such as lungs and heart increased roughly in line with the whole body, brain size did not increase significantly and was small relative to the body in *Grb10* KO pups. This correlates with the lack of expression from the *Grb10* maternal allele in the CNS, though interestingly no obvious effect on brain size at birth was seen in $Grb10^{+/p}$ pups and instead paternal *Grb10* expression in CNS has been associated with specific behavioural changes [24, 27–29]. In contrast to brain, $Grb10^{m/+}$ liver mass was at birth over twice that of wild type littermates [24–26]. This disproportionate enlargement was associated with excessive accumulation of lipid by hepatocytes whereas generally the excess growth involved changes in cell cycle and increased cell number during fetal development [26, 30]. Notably, skeletal muscle mass was increased at birth due to an increase in myofiber number, without changes in myofiber size or in the ratio of fast- and slow-twitch fibres [31], and this increase in muscle or lean mass persists into adulthood [26, 31–33].

Mice overexpressing *Grb10,* due to deletion of imprinting control regions that normally suppress expression of the paternally inherited allele, are born small (around 60% the mass of wild type littermates) and remain small into adulthood, modelling the situation in around 10-20% of growth restricted SRS patients who inherit two maternal copies of the chromosome 7 region containing *GRB10* [12, 13]. This illustrates a conserved role for *GRB10* in fetal growth control that is emphasized by genome-wide association studies in which *GRB10* has been linked with birth weight or body size in several mammalian populations, including human [34], pig [35], sheep [36]and Arctic ringed seal [37].

Mouse studies have shown that Grb10 regulates the Insr *in vivo* to influence glucose regulation through actions on peripheral tissues [19, 32, 38] and the endocrine pancreas [39], and are consistent with human population studies linking *GRB10* with energy homeostasis and endocrine pancreas function (e.g. [40]). Grb10 has also been shown to inhibit Igf1r activity in adult tissues [32, 39] and it is widely assumed that Grb10 influences fetal growth by acting on the Igf1r (Fig. 1B). We previously tested this assumption by performing crosses between *Grb10* KO and *Igf2* KO mouse mutants [25]. Resulting $Grb10^{m/+}$:$Igf2^{+/p}$ double knockout (DKO) pups were intermediate in size at birth, compared to $Grb10^{m/+}$ (large) and $Igf2^{+/p}$ (small) pups, indicating additive effects of two growth regulators acting largely independently of each other. Since both Igf1 and Igf2 influence fetal growth equally through the Igf1r [41–43] (Fig. 1A), these experiments formed only an indirect assessment of the potential for Grb10 to act via Igf1r. Given the unexpected nature of this result and the potential for some form of compensation occurring at the level of the receptor, here we tested directly for epistatic genetic interactions between *Grb10* and either *Igf1r* or *Insr*. We present two key findings. First, our data support the conclusion that Grb10 acts largely independently of Igf1r or Insr signaling to regulate fetal growth. Second, excessive lipid accumulation in the neonatal $Grb10^{m/+}$ liver was found to be *Insr*-dependent, meaning that Grb10 modulation of *Insr*-regulated metabolism begins during fetal development. These findings are important for the understanding of fetal growth regulation and its impact on tissue proportions and life-long metabolic health.

Results

Genetic interaction tests show that *Grb10* inhibits fetal growth independently of *Igf1r*

To directly assess the possibility that *Grb10* interacts with the *Igf1r* to influence growth we performed genetic crosses between both *Grb10Δ2-4* and *Grb10ins7* (collectively referred to as *Grb10* KO strains) and *Igf1r* KO mice. *Grb10Δ2-4* offspring were analysed at PN1 and e17.5 whereas *Grb10ins7* offspring were analysed at PN1 only. To increase statistical power, both sexes were pooled together and considered in a single analysis, with mean weights ± standard error of the mean stated in the text and shown graphically for offspring genotype groups. PN1 data were consistent between offspring of the two *Grb10* KO strains (as summarised in Table 1) and consequently all subsequent experiments were carried out with only the *Grb10Δ2-4* strain.

Grb10ins7 KO x Igf1r KO offspring PN1 body mass

Progeny of crosses between $Grb10ins7^{+/p}$:$Igf1r^{+/-}$ females and $Grb10ins7^{+/+}$:$Igf1r^{+/-}$ males were collected at PN1 for body and organ weight analysis (Fig. 2). Progeny with six genotypes were reduced to four groups by pooling $Grb10ins7^{+/+}$:$Igf1r^{+/-}$ with $Grb10ins7^{+/+}$:$Igf1r^{+/+}$ (wild type group) and $Grb10ins7^{m/+}$:$Igf1r^{+/-}$ and $Grb10in7^{m/+}$:$Igf1r^{+/+}$ (*Grb10ins7* KO group), for comparison with the *Igf1r* KO and *Grb10ins7*:*Igf1r* DKO groups (Table 2A). This was done following initial analysis of the data which confirmed that $Igf1r^{+/-}$ animals had a normal fetal growth phenotype (Additional file 1: Fig.S1), as previously shown [41]. Pooling allowed us to strengthen statistical analyses, while simplifying data analysis and presentation, without materially affecting the outcome. If Grb10 regulates growth through an interaction with the Igf1r, *Grb10*:*Igf1r*

Table 1 Summary of PN1 body and organ weight data for progeny of crosses between *Grb10* KO strains and *Igf1r* KO mice. Mean weights are shown for each genotype together with changes relative to wild type (%WT) for each mutant genotype. A) *Grb10ins7* KO data. B) *Grb10Δ2-4* KO data

	WT	*Igf1r* KO		*Grb10ins7* KO		DKO	
	Actual	Actual	%WT	Actual	%WT	Actual	%WT
A)							
Body	1.4010	0.6395	-54	1.7670	+26	1.1650	-17
Brain	0.0824	0.0491	-40	0.0860	+4	0.0535	-35
Liver	0.0550	0.0469	-15	0.1231	+124	0.1115	+103
Lung	0.0387	0.0079	-80	0.0480	+24	0.0287	-26
Heart	0.0092	0.0078	-15	0.0127	+39	0.0094	+2
Kidney	0.0159	0.0111	-31	0.0166	+5%	0.0128	-20
B)							
Body	1.422	0.6205	-56	1.887	+33	1.278	-10
Brain	0.0849	0.04953	-42	0.0931	+10	0.058	-32
Liver	0.0568	0.0454	-20	0.1279	+125	0.1259	+122
Lung	0.0398	0.0085	-79	0.0539	+35	0.0333	-16
Heart	0.0089	0.0073	-18	0.0134	+51	0.0112	+26
Kidney	0.0157	0.01	-36	0.0179	+14	0.0138	-12

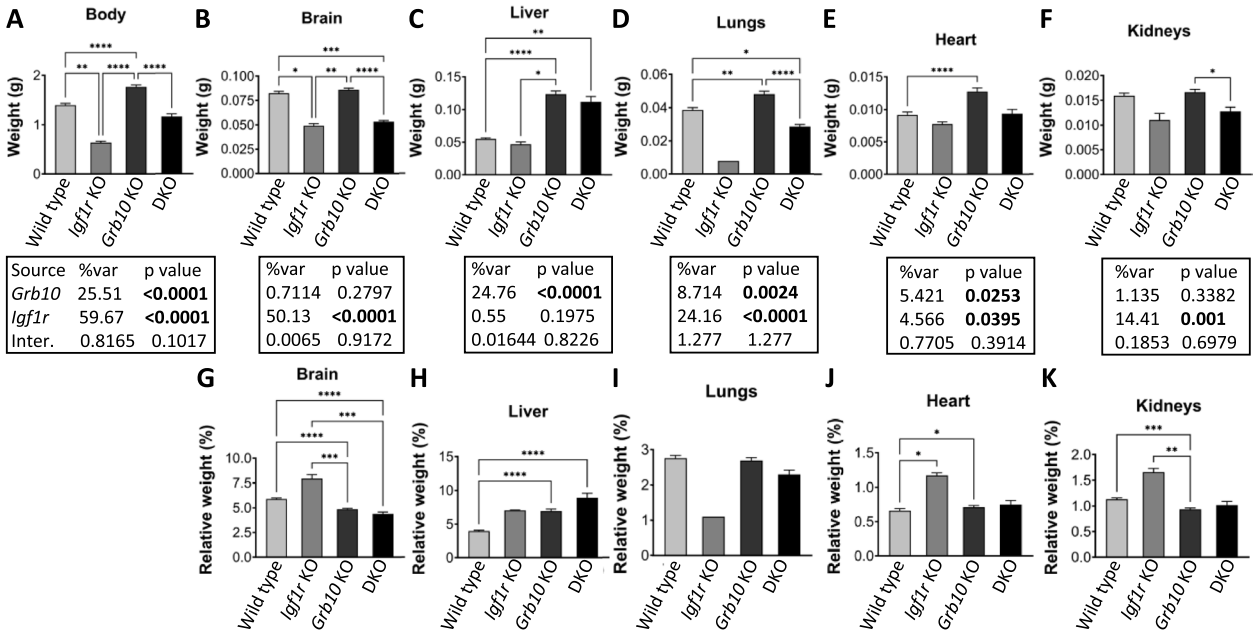

Fig. 2 Weights at PN1 from progeny of crosses between *Grb10ins7* KO and *Igf1r* KO mice. Data were pooled into four groups for analysis as described in the Methods, wild type, *Igf1r* KO, *Grb10* KO and *Grb10:Igf1r* double knockouts (DKO). Body weights are shown for the four offspring genotype groups (**A**). Actual weights of brain (**B**), liver (**C**), lungs (**D**), heart (**E**) and kidneys (**F**) are shown alongside relative weights of the same organs, expressed as a percentage of body mass (**G**-**K**). Values represent means and SEM, tested by one-way ANOVA using Kruskal-Wallis and Dunn's post hoc statistical tests. Summaries of Two-way ANOVA outcomes beneath each graph show the percentage of total variation (%var) and a *p* value for each source, namely the two single KO genotypes and any interaction (Inter.) between the two (values significant at $p<0.05$ in bold). Sample sizes were, for body, wild type (WT) $n=38$, *Igf1r* KO $n=7$, *Grb10* KO $n=26$, *Grb10:Igf1r* DKO $n=12$; brain, WT $n=38$, *Igf1r* KO $n=3$, *Grb10* KO $n=25$, *Grb10:Igf1r* DKO $n=8$; liver, WT $n=38$, *Igf1r* KO $n=2$, *Grb10* KO $n=25$, *Grb10:Igf1r* DKO $n=7$; lungs, WT $n=38$, *Igf1r* KO $n=7$, *Grb10* KO $n=12$, *Grb10:Igf1r* DKO $n=7$; heart, WT $n=37$, *Igf1r* KO $n=2$, *Grb10* KO $n=8$, *Grb10:Igf1r* DKO $n=7$; kidneys, WT $n=38$, *Igf1r* KO $n=2$, *Grb10* KO $n=25$, *Grb10:Igf1r* DKO $n=7$. Asterisks indicate *p*-values, $*p<0.05$, $**p<0.01$, $***p<0.001$, $****p<0.0001$

Table 2 Genetic crosses used in the study, showing parent and offspring genotypes with their expected Mendelian ratios. A) crosses between either *Grb10* KO strain, (*Grb10Δ2-4* and *Grb10ins7*) and the *Igf1r* KO strain. For statistical analysis $Igf1r^{+/-}$ heterozygous offspring were grouped with their respective $Igf1r^{+/+}$ wild type counterparts, as indicated. B) Crosses between the *Grb10Δ2-4* KO and *Insr* KO strains. For statistical analysis $Insr^{+/-}$ heterozygous offspring were grouped with their respective $Insr^{+/+}$ wild type counterparts, $Grb10^{+/p}$ with respective $Grb10^{+/+}$ wild types and $Grb10^{m/p}$ with respective $Grb10^{m/+}$ as *Grb10* maternal allele knockouts, as indicated. DKO = double knockout

A)						
Parents	$Grb10^{+/p}$: $Igf1r^{+/-}$ female x $Igf1r^{+/-}$ male (separate crosses were made using the *Grb10Δ2-4* and *Grb10ins7* strains)					
Offspring	$Grb10^{+/+}$: $Igf1r^{+/+}$	$Grb10^{+/+}$: $Igf1r^{+/-}$	$Grb10^{+/+}$: $Igf1r^{-/-}$	$Grb10^{m/+}$: $Igf1r^{+/+}$	$Grb10^{m/+}$: $Igf1r^{+/-}$	$Grb10^{m/+}$: $Igf1r^{-/-}$
Ratio	1	2	1	1	2	1
Group	Wild type		*Igf1r* KO	*Grb10* KO		*Grb10*:*Igf1r* DKO
B)						
Parents	$Grb10^{+/p}$: $Insr^{+/-}$ female x $Grb10^{+/p}$: $Insr^{+/-}$ male (only crosses involving the *Grb10Δ2-4* strain were made)					
Offspring	$Grb10^{+/+}$: $Insr^{+/+}$	$Grb10^{+/+}$: $Insr^{+/-}$	$Grb10^{+/+}$: $Insr^{-/-}$	$Grb10^{m/+}$: $Insr^{+/+}$	$Grb10^{m/+}$: $Insr^{+/-}$	$Grb10^{m/+}$: $Insr^{-/-}$
Ratio	1	2	1	1	2	1
	$Grb10^{+/p}$: $Insr^{+/+}$	$Grb10^{+/p}$: $Insr^{+/-}$	$Grb10^{+/p}$: $Insr^{-/-}$	$Grb10^{m/p}$: $Insr^{+/+}$	$Grb10^{m/p}$: $Insr^{+/-}$	$Grb10^{m/p}$: $Insr^{-/-}$
Ratio	1	2	1	1	2	1
Group	Wild type		*Insr* KO	*Grb10* KO		*Grb10*:*Insr* DKO

DKO animals would be expected to be phenotypically indistinguishable from *Igf1r* KO animals (Fig. 1B). Body mass data (Fig. 2A; Table 1A) immediately indicated that we should reject this hypothesis. *Grb10ins7* KO pups (mean weight 1.7670±0.0360g) were approximately 26% larger ($p<0.0001$) and *Igf1r* KOs (0.6395±0.0267g) 54% smaller ($p<0.01$) than wild type controls (1.401±0.0297g), respectively, whereas *Grb10ins7*:*Igf1r* DKO mutants were intermediate in size (1.1650±0.0554g). Thus, *Grb10ins7*:*Igf1r* DKO pups displayed an additive effect of both parental genotypes, being significantly different from *Grb10ins7* KO ($p<0.0001$) single mutants, but not from both *Igf1r* KOand wild type neonates (Fig. 2A). This was supported by a two-way ANOVA test which showed both *Grb10* ($p<0.0001$) and *Igf1r* ($p<0.0001$) are significant factors affecting body weight, in opposite directions, but detected no interaction between the two genotypes ($p=0.1017$).

Grb10ins7 KO x Igf1r KO offspring PN1 organ mass

To assess body proportions selected individual organs (brain, liver, lungs, heart, kidneys) were dissected at PN1 and their weights were analysed directly (Fig. 2B-F) and as a percentage of total body weight (Fig. 2G-K). The pattern of organ weight difference across the genotypes was again consistent with the DKO pups having an additive phenotype, comprising the sum of the two single KO phenotypes (summarised in Table 1A). First, the brain from *Grb10ins7* KO (mean mass 0.0860±0.0017g) pups was spared from the general overgrowth phenotype indicated by body mass and was only 4% larger than wild type brain (0.0824±0.0019g) (Fig. 2B). Meanwhile, brains from *Igf1r* KO (0.0491±0.0021g) and *Grb10ins7*:*Igf1r* DKO (0.0535±0.0012g) pups were strikingly similar, being smaller than wild type brain by 40% ($p<0.05$), and 35% ($p<0.001$), respectively. Thus, while *Igf1r* KO brains were roughly proportionate with body size, both *Grb10ins7* KO ($p<0.0001$) and *Grb10ins7*:*Igf1r* DKO ($p<0.0001$) brains were disproportionately small within larger bodies (Fig. 2G). In other words, the *Grb10ins7*:*Igf1r* DKO phenotype was dominated by brain size being severely reduced, as in *Igf1r* KO pups, which can therefore be attributed to loss of *Igf1r* expression. In keeping with this Two-way ANOVA indicated that brain weight was influenced mainly by *Igf1r* ($p<0.0001$).

In direct contrast, the livers of *Grb10ins7* KO (0.1231± 0.0051g) and *Grb10ins7*:*Igf1r* DKO (0.1115±0.0083g) pups were each at least double, by 124% ($p<0.0001$) and 103% ($p<0.01$), respectively, the size of wild type (0.0550±0.0016g), while the *Igf1r* KO (0.0469±0.0036g) liver was some 15% smaller (Fig. 2C). Consequently, while the liver was disproportionately enlarged within the heavier *Grb10ins7* KO body ($p<0.0001$), liver disproportion was exaggerated in *Grb10ins7*:*Igf1r* DKO ($p<0.0001$) pups, due to DKOs having a body size similar to wild type (Fig. 2H). Due to their greatly reduced body mass relative to wild types, although *Igf1r* KO livers were smaller in actual mass than in wild type controls, *Igf1r* KO pups also had disproportionately large livers. Although neither actual nor relative liver weight was significantly different between *Igf1r* KO and wild type (likely due to the small Igf1r KO small sample size), the *Grb10ins7*:*Igf1r* DKO liver weight phenotype was clearly dominated by the

massive size increase also seen in *Grb10* KO single mutants and therefore associated with loss of the maternal *Grb10ins7* allele. Two-way ANOVA analysis reflected this with only *Grb10* significantly (p<0.0001) contributing to liver weight.

The remaining organs followed a pattern of size difference like that seen in the body mass data, in that *Grb10ins7*:*Igf1r* DKO mass was intermediate between that of the two single KO values. Compared to wild type (0.0387±0.0014g) lungs from a single *Igf1r* KO sample (0.0079g) were 80% lighter (not statistically significant due to very small samples size) and *Grb10ins7* KO (0.0480±0.0019g) 24% heavier (p<0.01), whereas *Grb10ins7*:*Igf1r* DKO (0.0287±0.0013g) lungs were 26% smaller (p<0.05) and intermediate in size (Fig. 2D). Relative to total body mass, *Igf1r* KO lungs appeared disproportionately small while *Grb10ins7* KO and *Grb10ins7*:*Igf1r* DKO lungs were roughly proportionate with their respective body sizes (F igure 2I). According to two-way ANOVA, both *Grb10* (p<0.0024) and *Igf1r* (p<0.0001) contributed significantly to lung weight. Similarly, in comparison with wild type (0.0092±0.0005g), hearts from *Igf1r* KO (0.0078±0.0004g) pups were some 15% smaller and *Grb10ins7* KO hearts (0.0127±0.0006g) 39% larger (p<0.0001), with *Grb10ins7*:*Igf1r* DKO hearts (0.0094±0.0006g), intermediate in size, being only 2% larger than wild type (Fig. 2E). While these weight differences were not all statistically significant, in relative terms, the heart from *Grb10ins7* KO (p<0.05) and *Igf1* KO (p<0.05) single mutants were disproportionately large, whereas the *Grb10ins7*:*Igf1r* DKO heart was not (Fig. 2J). Two-way ANOVA indicated *Igf1r* (p<0.0395) as the major contributor to heart weight.

In the case of kidneys, those from *Grb10ins7* KO (0.0166±0.0006g) were only slightly enlarged, by 5%, compared with wild type (0.0159±0.0005g), while both *Igf1r* KO (0.0111±0.00134g) and DKO (0.01287±0.0009g), were smaller by 31% and 20%, respectively (Fig. 2F). The only significant difference in kidney weights was between *Grb10ins7* KO and *Grb10ins7*:*Igf1r* DKO (p<0.05). Relative to wild type body mass, this meant that *Grb10ins7* KO pups alone had disproportionately small kidneys (p<0.001) (Fig. 2K). Two-way ANOVA indicated *Igf1r* (p<0.001) as the major contributor to kidney weight. For each individual organ two-way ANOVA tests indicated there was no interaction between the genotypes, just as for the whole body (Fig. 2A-F).

Grb10Δ2-4 KO x Igf1r KO offspring PN1 body mass

To corroborate data from the *Grb10ins7* strain, similar PN1 data were collected using the *Grb10Δ2-4* strain. Progeny of crosses between *Grb10Δ2-4*$^{+/p}$:*Igf1r*$^{+/-}$ females and *Grb10Δ2-4*$^{+/+}$:*Igf1r*$^{+/-}$ males were again collected at PN1 and whole body weights recorded along with weights of selected organs (Fig. 3). As before, data for the six offspring genotypes were pooled to generate four groups for analysis, combining *Grb10Δ2-4*$^{+/+}$:*Igf1r*$^{+/-}$ with *Grb10Δ2-4*$^{+/+}$:*Igf1r*$^{+/+}$ (wild type group) and *Grb10Δ2-4*$^{m/+}$:*Igf1r*$^{+/-}$ with *Grb10Δ2-4*$^{m/+}$:*Igf1r*$^{+/+}$ (*Grb10Δ2-4* KO group) progeny (Table 1B), which was again supported by our initial data analysis (Additional file 1: Fig. S2). As for the previous cross, while *Grb10Δ2-4* KO pups (mean weight 1.887 ±0.0239g) were around 33% larger (p<0.0001) and *Igf1r* KOs (0.6205±0.0192g) 56% smaller (p<0.001), respectively, than wild type controls (1.422±0.0189g), *Grb10Δ2-4:Igf1r* DKO mutants (1.278±0.0381g) were intermediate in size, just 10% smaller than wild type (Fig. 3A; Table 1B). *Grb10Δ2-4:Igf1r* DKO pups were smaller than *Grb10Δ2-4* KO pups (p<0.0001) but not significantly smaller than wild type neonates (Fig. 3A, B), while *Grb10Δ2-4* KO pups were significantly larger than both wild type (p<0.0001) and *Igf1r* KO (p<0.0001) pups. The two-way ANOVA test showed both *Grb10* (p<0.0001) and *Igf1r* (p<0.0001) contributed significantly to body weight and indicated a possible interaction between the genotypes, but at a relatively high significance level (p=0.0135). Despite this, it was clear that *Grb10Δ2-4:Igf1r* DKO pups were not small, to the extent consistently shown for *Igf1r* KO pups, and instead their intermediate size must result from an additive effect of the two mutant parental genotypes.

Grb10Δ2-4 KO x Igf1r KO offspring PN1 organ mass

As before, body proportions were assessed by dissecting and weighing selected organs at PN1. Organ weights were analysed directly (Fig. 3C-G) and as a percentage of total body weight (Fig. 3H-L). The genotype-dependent differences in organ weights were again consistent with the *Grb10Δ2-4:Igf1r* DKO pups having an additive phenotype in comparison with the two single KO genotypes (summarised in Table 1B). First, the brain from *Grb10Δ2-4* KO (0.0931±0.001g) pups was spared from the general overgrowth phenotype indicated by body mass and was only 10% larger (p<0.0001) than wild type brain (0.0849±0.0011g) (Fig. 3C), Meanwhile, brains from *Igf1r* KO (0.058±0.0018g) and *Grb10Δ2-4:Igf1r* DKO (0.058±0.0012g) pups were strikingly similar, being smaller than wild type brain by 42%, (p<0.01) and 32% (p<0.0001), respectively. Thus, while *Igf1r* KO brains were proportionate to their small bodies, both *Grb10Δ2-4* KO (p<0.0001) and *Grb10Δ2-4:Igf1r* DKO (p<0.0001) brains were small within larger bodies (Fig. 3H). In other words, the *Grb10Δ2-4:Igf1r* DKO phenotype was dominated by brain size being severely reduced, as in *Igf1r* KO pups, and is therefore associated with loss of *Igf1r* expression.

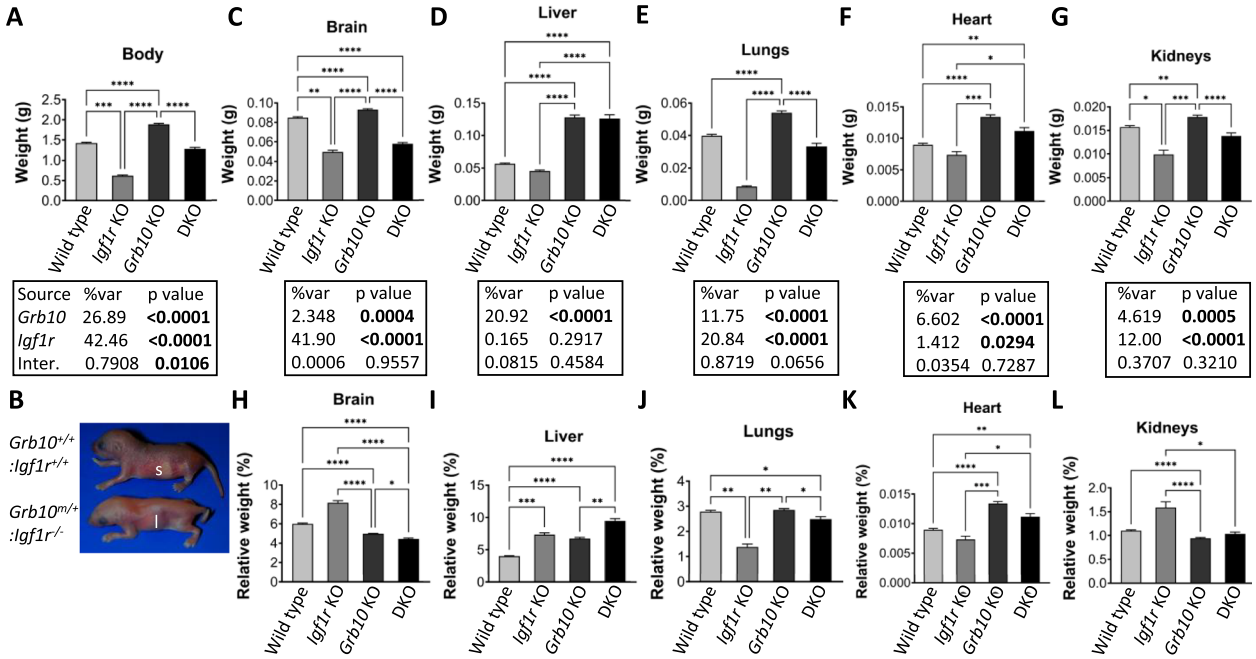

Fig. 3 Weights at PN1 from progeny of crosses between *Grb10Δ2-4* KO and *Igf1r* KO mice. Data were pooled into four groups for analysis as described in the Methods, wild type, *Igf1r* KO, *Grb10* KO and *Grb10:Igf1r* double knockouts (DKO). Body weights are shown for the four offspring genotype groups (**A**). Gross physical appearance of typical WT (*Grb10*$^{+/+}$*:Igf1r*$^{+/+}$) and *Grb10:Igf1r* DKO (*Grb10*$^{-/-}$*:Igf1r*$^{-/-}$) pups, noting in the DKO the small head relative to body size and enlarged liver (l) obscuring the milk filled stomach (s), clearly visible through the skin of the wild type (**B**). Actual weights of brain (**C**), liver (**D**), lungs (**E**), heart (**F**) and kidneys (**G**) are shown alongside relative weights of the same organs, expressed as a percentage of body mass (**H**-**L**). Values represent means and SEM, tested by one-way ANOVA using Kruskal-Wallis and Dunn's post hoc statistical tests. Summaries of Two-way ANOVA outcomes beneath each graph show the percentage of total variation (%var) and a *p* value (values significant at $p<0.05$ in bold) for each source, namely the two single KO genotypes and any interaction (Inter.) between the two. Sample sizes were, for body wild type (WT) $n=104$, *Igf1r* KO $n=13$, *Grb10* KO $n=92$, *Grb10:Igf1r* DKO $n=28$; brain, WT $n=102$, *Igf1r* KO $n=6$, *Grb10* KO $n=90$, *Grb10:Igf1r* DKO $n=24$; liver, WT $n=104$, *Igf1r* KO $n=5$, *Grb10* KO $n=90$, *Grb10:Igf1r* DKO $n=23$; lungs, WT $n=104$, *Igf1r* KO $n=4$, *Grb10* KO $n=90$, *Grb10:Igf1r* DKO $n=23$; heart, WT $n=103$, *Igf1r* KO $n=5$, *Grb10* KO $n=88$, *Grb10:Igf1r* DKO $n=23$; kidneys, WT $n=100$, *Igf1r* KO $n=5$, *Grb10* KO $n=90$, *Grb10:Igf1r* DKO $n=23$. Asterisks indicate *p*-values, *$p<0.05$, **$p<0.01$, ***$p<0.001$, ****$p<0.0001$

In contrast, the livers of DKO (0.1259±0.006g) and *Grb10Δ2-4* KO (0.1279±0.0036g) pups were again each more than double (122% and 127% larger, respectively) the size of wild type (0.0568±0.0012g) liver ($p<0.0001$), while the *Igf1r* KO (0.0454±0.0016g) liver was some 20% smaller (Fig. 3D). Consequently, the liver was disproportionately enlarged within the heavier *Grb10Δ2-4* KO body ($p<0.0001$), and in the *Grb10Δ2-4:Igf1r* DKO liver disproportion was exaggerated ($p<0.0001$), due to DKOs having a body size similar to wild type (Fig. 3I). Due to their greatly reduced body mass relative to wild types, although *Igf1r* KO livers were smaller in actual mass than in wild type controls, *Igf1r* KO pups also had disproportionately large livers ($p<0.001$). Similar to our findings using the *Grb10ins7* KO strain, the *Grb10Δ2-4:Igf1r* DKO phenotype was clearly dominated by the massive size increase associated with loss of the maternal *Grb10Δ2-4* allele.

The remaining organs followed a pattern of size differences like that seen in the body mass data, in that DKO mass was intermediate between that of the two single KO values. Lungs from *Grb10Δ2-4:Igf1r* DKO (0.0333±0.0018g) pups were only 16 % smaller than wild type (0.0398±0.0009g) but differed to those of both single mutants, with *Igf1r* KO (0.0085±0.0005g) approximately 79% lighter than wild type and *Grb10Δ2-4* KO (0.0539±0.0012g) 35% heavier ($p<0.0001$) (Fig. 3E). *Grb10Δ2-4* KO lung weight was significantly different to all three other genotypes ($p<0.0001$ in each case).. Relative to total body mass, *Igf1r* KO lungs were disproportionately small ($p<0.01$) while *Grb10Δ2-4* KO lungs were roughly proportionate with their respective body sizes and *Grb10Δ2-4:Igf1r* DKO marginally ($p<0.05$), disproportionately small (Fig. 3J). Similarly, in comparison with wild type (0.009±0.0002g), hearts from *Igf1r* KO (0.0073±0.0005g) pups were some 18% smaller and *Grb10Δ2-4* KO hearts (0.0134±0.0003g) 51% larger ($p<0.0001$) (Fig. 3F). *Grb10Δ2-4:Igf1r* DKO hearts (0.0112±0.0005g) were intermediate in size, being 26% larger ($p<0.01$) than wild type but not significantly

different to *Grb10* KO single mutants In relative terms, the hearts from *Igf1r* KO pups were proportionate and those of *Grb10* KO (p<0.0001) and DKO (p<0.01) of *Grb10* KO (p<0.0001) and DKO (p<0.01) disproportionately large compared to wild type controls. (Fig. 3K).

Compared to wild type kidneys (0.0157±0.0003g), *Igf1r* KO (0.0099±0.0009g) kidneys were reduced in size, by 36% (p<0.05), while *Grb10Δ2-4* KO kidneys (0.0179±0.0004g) were larger by 14% (p<0.01) and *Grb10Δ2-4:Igf1r* DKO (0.0138±0.0006g) were intermediate, being 12% larger, but not significantly different to wild type (Fig. 3G). Notably, *Grb10Δ2-4* KO kidney weights were still significantly different to those of *Igf1r* KO (p<0.001) and *Grb10Δ2-4:Igf1r* DKO (p<0.0001). Relative to body mass (Fig. 3L), this meant kidneys were proportionate in *Igf1r* KO pups, but disproportionately small in the larger body of *Grb10Δ2-4* KO (p<0.0001) pups. As in the previous cross, two-way ANOVA tests for individual organs indicated there was no interaction between the genotypes in each case (Fig. 3C-G). In almost all cases both *Grb10* and *Igf1r* contributed significantly to organ weight. The exception was liver where *Grb10* (p<0.0001) was the major influence on weight and the influence of *Igf1r* did not reach significance.

The organ disproportion evident in *Grb10Δ2-4:Igf1r* DKO PN1 pups was reflected by their appearance (Fig. 3B). Despite being similar in size to wild types, *Grb10Δ2-4:Igf1r* DKO pups had small, flattened heads and livers that were distended such that they largely obscured the milk-filled stomach.

Grb10Δ2-4 KO x Igf1r KO offspring e17.5 embryo and placenta

To investigate the potential for interaction between *Igf1r* and *Grb10* to regulate growth by acting within the placenta we analysed weights of the whole embryo and placenta at e17.5 (Fig. 4). We chose a time-point late in gestation when any size differences between conceptuses of different genotypes would be relatively large. The pattern of size differences observed was very similar to that seen for pups at PN1. *Grb10Δ2-4* KO embryos (1.085±0.0450g) were 35% larger than wild type (0.8031±0.0371g), whereas the single *Igf1r* KO (0.4029g) embryo collected was 50% smaller and *Grb10Δ2-4:Igf1r* DKO embryos (0.6330±0.0286g) intermediate in size, at 21% lighter than wild types (Fig. 4A). Unsurprisingly, the one *Igf1r* KO embryo showed no statistical differences in size compared to any of the other genotypes, however, *Grb10Δ2-4* KO embryos were significantly larger than wild type (p<0.05) and *Grb10Δ2-4:Igf1r* DKO (p<0.0001) embryos.

Placental weights followed a similar pattern (Fig. 4B), with *Grb10Δ2-4* KO (0.1073±0.0060g) 22% larger than wild type (0.0882±0.0036g), the single *Igf1r* KO placenta (0.0729g) 17% smaller and *Grb10Δ2-4:Igf1r* DKO placentas (0.0916±0.0040g) in between at only 4% larger. The only statistically significant difference was between wild type and *Grb10Δ2-4* KO samples (p<0.05). Next, the ratio of embryo to placental mass was calculated for each genotype as an estimate of placental efficiency (Fig. 4C). Although not statistically significant, the trend

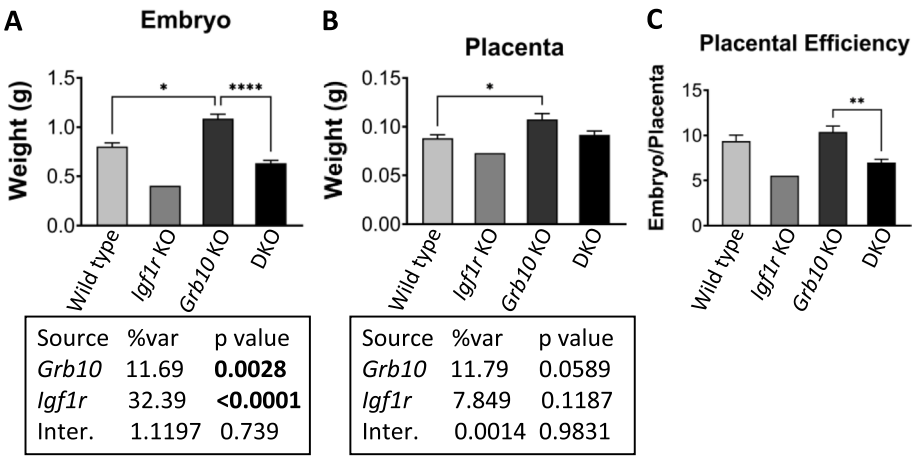

Source	%var	p value
Grb10	11.69	**0.0028**
Igf1r	32.39	**<0.0001**
Inter.	1.1197	0.739

Source	%var	p value
Grb10	11.79	0.0589
Igf1r	7.849	0.1187
Inter.	0.0014	0.9831

Fig. 4 Weight analysis of e17.5 conceptuses from crosses between *Grb10Δ2-4* KO and *Igf1r* KO mice. Data were pooled into four groups for analysis as described in the Methods, wild type, *Igf1r* KO, *Grb10* KO and *Grb10:Igf1r* double knockouts (DKO). Weights are shown for the four offspring genotype groups for embryo (**A**) and placenta (**B**) and these have been used to calculate the embryo:placenta weight ratio as a measure of placental efficiency (**C**). Values represent means and SEM, tested by one-way ANOVA using Kruskal-Wallis and Dunn's post hoc statistical tests. Summaries of Two-way ANOVA outcomes beneath each graph show the percentage of total variation (%var) and a p value (values significant at p<0.05 in bold) for each source, namely the two single KO genotypes and any interaction (Inter.) between the two. Sample sizes were, for wild type (WT) n=17, *Igf1r* KO n=1, *Grb10* KO n=11, *Grb10:Igf1r* DKO n=9. Asterisks indicate p-values, *p <0.05, **p <0.01, ****p<0.0001

was for *Grb10Δ2-4* KO placental efficiency (10.41) to be slightly higher than wild type (9.39), while both *Igf1r* KO (5.53) and *Grb10Δ2-4:Igf1r* DKO (6.98) were lower than wild type, with the only significant difference between *Grb10Δ2-4* KO and *Grb10Δ2-4:Igf1r* DKO ($p<0.01$). A two-way ANOVA test found no evidence of an interaction between the genotypes for either embryo or placenta size (Fig. 4A,B).

Survival of Grb10 KO x Igf1r KO progeny at PN1 and e17.5

During collection of offspring the small, presumptive *Igf1r* KO pups seemed scarce and chi-square tests of observed versus expected numbers generally supported this notion (Additional file 2: Table S1). Testing of PN1 data from the *Grb10Δ2-4* KO x *Igf1r* KO cross, which had the largest sample size ($n=237$), indicated that paucity of *Igf1r* KO pups was statistically significant ($p=0.0174$; Additional file 2: Table S1A), with 44% of the expected numbers surviving. The same was true for offspring collected from the same cross at e17.5 ($p=0.015$), though in this case the sample size was lower ($n=38$) and only one *Igf1r KO* embryo was obtained, with the expected number being closer to 5 (Additional file 2: Table S1B). In the case of the *Grb10ins7* x *Igf1r* KO PN1 dataset ($n=83$), the lack of *Igf1r* KO pups was less evident (67% of the expected number) and the chi-square test indicated no significant deviation from expected mendelian ratios ($p=0.4711$; Additional file 2: Table S1C). In both crosses it was clear that *Igf1r* KO pups found alive on the day of birth were failing to thrive, as previously reported [42]. Strikingly, this did not appear to be true for *Grb10:Igf1r* DKO PN1 pups in either cross which typically had milk-filled stomachs, appeared to be doing well on PN1 and were not underrepresented (Additional file 2: Table S1).

Genetic interaction tests show that *Grb10* inhibits fetal growth largely independently of the *Insr*, except in liver, where excessive enlargement in *Grb10* KO neonates is due to *Insr*-mediated lipid accumulation

Grb10Δ2-4 KO x Insr KO offspring PN1 body mass

To address the question of whether *Grb10* regulates growth *in vivo* through an interaction with the *Insr*, we next performed intercrosses between *Grb10Δ2-4*$^{+/p}$:*Insr*$^{+/-}$ double heterozygous mice, giving rise to twelve offspring genotypes, which were reduced to four groups for analysis (Table 2B). In addition to combining animals with *Insr*$^{+/-}$ and *Insr*$^{+/+}$ genotypes (*Insr* wild type groups), we also pooled *Grb10Δ2-4*$^{+/+}$ with *Grb10Δ2-4*$^{+/p}$ genotypes (*Grb10* wild type) and *Grb10Δ2-4*$^{m/+}$ with *Grb10Δ2-4*$^{m/p}$ (*Grb10* KO). This is because the *Grb10* paternal allele is silent in the majority of tissues and its knockout is well established to have no effect on fetal growth [24–26, 49]. Similarly, only *Insr*$^{-/-}$ animals have been shown to have a mutant phenotype affecting either growth or glucose regulation [43, 45, 50]. Initial analysis of our data prior to pooling was in line with these earlier studies (Additional file 1: Fig. S3). As asserted in the case of the Igf1r, should Grb10 regulate growth through an interaction with the Insr, *Grb10Δ2-4:Insr* DKO animals would be phenotypically indistinguishable from *Insr* KO single mutants (Fig. 1B).

Progeny were first collected at PN1 for body and organ weight analysis (Fig. 5). Just like the crosses involving the *Igf1r* KO, body mass data (Fig. 5A, Table 3) indicated that we should reject this hypothesis for crosses involving the *Insr*. *Insr* KO pups (1.2680±0.0483g) were not significantly different to wild type controls (1.3440±0.0297g), being only 6% smaller. In contrast, both *Grb10Δ2-4* KO (1.8140±0.0447g) and *Grb10Δ2-4:Insr* DKO (1.6990±0.0853g) pups were substantially larger than wild type, by 35% ($p<0.0001$) and 26% ($p<0.05$), respectively, but not significantly different to each other. Thus, the overgrowth associated with loss of the maternal *Grb10* allele is maintained in DKO pups despite loss of *Insr* expression. A two-way ANOVA test supported this, showing that body weight was mostly driven by *Grb10* ($p<0.0001$) with little influence from *Insr*, and no evidence of an interaction between the genotypes (Fig. 5A).

Grb10Δ2-4 KO x Insr KO offspring PN1 organ mass

As for the earlier crosses involving *Igf1r* KO strains, the same selection of organs was collected and weighed at PN1 to evaluate body proportions of offspring involving the *Insr* KO. Organ weights were analysed directly (Fig. 5B-F) and as a percentage of total body weight (Fig. 5G-K). The patterns of weight differences displayed across the genotypes was consistent with the *Grb10Δ2-4:Insr* DKO pups having an additive phenotype compared with the two single KOs (summarised in Table 3). The brain from *Grb10Δ2-4* KO (0.0918±0.0014g) pups was once again largely spared from the general overgrowth phenotype indicated by body mass, being only 9% larger than wild type (0.0841±0.0014g), which was a significant difference ($p<0.001$) in this cross (Fig. 5B). Brains from *Grb10Δ2-4:Insr* DKO (0.0930±0.0044g) pups were similarly some 11% larger than wild type, whereas *Insr* KO brains (0.0856±0.0039g) were almost indistinguishable at only 2% larger. This meant that *Grb10Δ2-4* KO and *Grb10Δ2-4:Insr* DKO brains were disproportionately small within larger bodies (Fig. 5G), compared with wild type ($p<0.0001$ and $p<0.05$, respectively) and *Insr* KO ($p<0.0001$ and $p<0.05$) brains. Thus, *Grb10Δ2-4:Insr* DKO brain size followed the pattern of the *Grb10Δ2-4* KO and not the *Insr* KO single mutant phenotype. This interpretation is supported by two-way ANOVA which showed *Grb10* ($p<0.0074$), but not *Insr* to be a significant influence on brain weight.

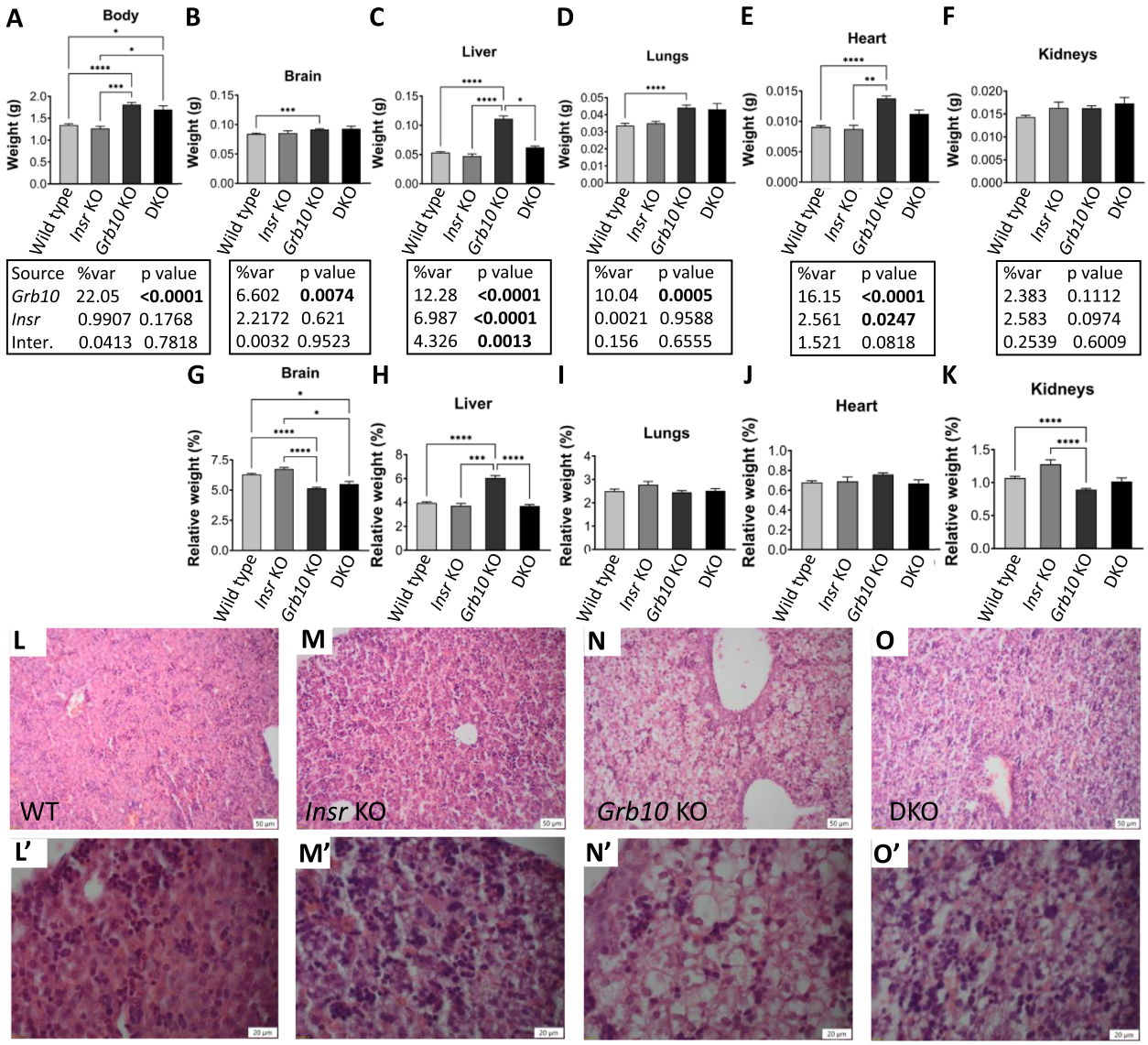

Fig. 5 Analyses of PN1 progeny from crosses between *Grb10Δ2-4* KO and *Insr* KO mice. Data for numerical analyses were pooled into four groups for analysis as described in the Methods, wild type (WT), *Insr* KO (IKO), *Grb10* KO (GKO) and *Grb10*:*Insr* double knockouts (DKO). Body weights are shown for the four offspring genotype groups (**A**). Actual weights of brain (**B**), liver (**C**), lungs (**D**), heart (**E**) and kidneys (**F**) are shown alongside relative weights of the same organs, expressed as a percentage of body mass (**G**-**K**). Values represent means and SEM, tested by one-way ANOVA using Kruskal-Wallis and Dunn's post hoc statistical tests. Summaries of Two-way ANOVA outcomes beneath each graph show the percentage of total variation (%var) and a p value (values significant at $p<0.05$ in bold) for each source, namely the two single KO genotypes and any interaction (Inter.) between the two. Sample sizes were, wild type (WT) $n=42$, *Insr* KO $n=6$, *Grb10* KO $n=44$, *Grb10*:*Insr* DKO $n=9$. Histological sections of liver, stained with haematoxylin and eosin, are shown at 100x magnification for WT (**L**), *Insr* KO (**M**), *Grb10* KO (**N**) and *Grb10*:*Insr* DKO (**O**) mice, and at 300x magnification for the same animals (**L'**-**O'**). Images are representative of at least three biological replicates per genotype and were taken at 100x magnification (scale bars show 50μm for the lower power images and 20μm for the higher power images). Asterisks indicate *p*-values, *$p<0.05$, **$p<0.01$, ***$p<0.001$, ****$p<0.0001$

Liver displayed a particularly interesting pattern of weight differences (Fig. 5C). Wild type (0.0533±0.0017g) and *Insr* KO (0.0475±0.0036g) liver sizes were very similar, while *Grb10Δ2-4* KO (0.1112±0.0049g) liver was more than twice normal size, at 109% larger than wild type ($p<0.0001$), as seen in the previous crosses. However, in this case *Grb10Δ2-4*:*Insr* DKO liver (0.0622±0.0023g) was only 17% larger than wild type and was significantly different to *Grb10Δ2-4* KO liver size ($p<0.05$) but not to wild type or *Insr* KO liver, indicating that the disproportionate liver overgrowth associated with loss of *Grb10* expression was largely Insr-dependent. This conclusion

Table 3 Summary of PN1 body and organ weight data for progeny of crosses between the *Grb10Δ2-4* KO strain and *Insr* KO mice. Mean weights are shown for each genotype together with changes relative to wild type (%WT) for each mutant genotype

	WT	*Insr* KO		*Grb10Δ2-4* KO		DKO	
	Actual	Actual	%WT	Actual	%WT	Actual	%WT
Body	1.3440	1.2680	-6	1.8140	+35	1.6990	+26
Brain	0.0841	0.0856	+2	0.0918	+9	0.0930	+11
Liver	0.0533	0.0475	-11	0.1112	+109	0.0622	+17
Lung	0.0337	0.0350	+4	0.0442	+31	0.0431	+28
Heart	0.0091	0.0087	-4	0.01378	+51	0.0112	+23
Kidney	0.0143	0.0163	+14	0.0163	+14	0.0173	+21

was reinforced by the finding that only *Grb10Δ2-4* KO liver was disproportionately enlarged, in comparison with wild type ($p<0.0001$), *Insr* KO ($p<0.001$) and *Grb10Δ2-4:Insr* DKO ($p<0.0001$) (Fig. 5H). Further, a two-way ANOVA test found an interaction between the genotypes for liver weight ($p=0.0013$) but not for any other organ (Fig. 5A-F). To investigate the liver phenotype further we carried out histological analysis and found that the accumulation of excess lipid previously observed in neonatal *Grb10Δ2-4* KO pups [26] was abrogated in *Grb10Δ2-4:Insr* DKO pups. Viewed at lower magnification (100x), the enlargement of hepatocytes through excess lipid storage was seen throughout *Grb10Δ2-4* KO (Fig. 5N), but not wild type (Fig. 5L), *Insr* KO (Fig. 5M) or *Grb10Δ2-4:Insr* DKO (Fig. 5O) liver sections. A degenerate fatty histopathological phenotype, that has previously been described in neonatal liver of *Insr* KO homozygotes [45, 50], is seen more clearly at higher magnification (300x) (Fig. 5M'). This was also evident in *Grb10Δ2-4:Insr* DKO (Fig. 5O') sections, is distinct from the lipid engorged cellular phenotype of *Grb10Δ2-4* KO liver (Fig. 5N') and absent in wild type sections (Fig. 5L'). Thus, the disproportionate hepatic overgrowth in *Grb10* KO neonates was due to Insr signalling-dependent lipid deposition.

Lungs and heart followed a pattern of size differences like that of body mass. *Grb10Δ2-4* KO (0.0442±0.0015g) and *Grb10Δ2-4:Insr* DKO (0.0431±0.0034g) lungs were similar in size, being 31% ($p<0.0001$) and 28% larger, respectively than wild type (0.0337±0.0013g), whereas *Insr* KO (0.0350±0.0011g) lungs were only 4% larger (Fig. 5D). Lungs from animals of all four genotypes remained proportionate with body weight (F igure 5I). Similarly, *Grb10Δ2-4* KO (0.01378±0.0004g) and *Grb10Δ2-4:Insr* DKO (0.0112±0.0006g) hearts were both larger than wild type (0.0091±0.0002g) hearts by 51% ($p<0.0001$) and 23%, respectively, while *Insr* KO (0.0087±0.0006g) hearts were 4% smaller and indistinguishable from wild type (Fig. 5E). Hearts from animals of all four genotypes were proportionate with body weight (Fig. 5J). In this cross, *Grb10Δ2-4* KO (0.0163±0.0005g) kidneys were 14% larger than wild type (0.0143±0.0004g) (Fig. 5F) but remained disproportionately small ($p<0.0001$) (Fig. 5K). Conversely, *Insr* KO (0.0163±0.0013g) kidneys were 14% larger than wild type and disproportionately large. *Grb10Δ2-4:Insr* DKO (0.0173±0.0013g) kidneys were 21% larger than wild type controls and roughly proportionate such that relative to body mass they were intermediate between the two single KOs. This once again reinforced the sparing of kidneys from the general overgrowth associated with loss of the maternal *Grb10* allele.

Grb10Δ2-4 KO x Insr KO offspring e17.5 embryo and placenta

We next investigated the potential for interaction between *Insr* and *Grb10* within the placenta by analysing weights of the whole embryo and placenta at e17.5 (Fig. 6). Similar to pups at PN1, compared to wild types (0.9245±0.0240g), *Insr* KO (0.8034±0.0569g) embryos were 13% smaller, though not significantly so, whereas *Grb10Δ2-4* KO embryos (1.3010±0.0445g) and *Grb10Δ2-4:Insr* DKO embryos (1.2130±0.0741g) were larger, by 41% ($p<0.0001$) and 31%, respectively (Fig. 6A). This meant *Grb10Δ2-4* KO ($p<0.0001$) and *Grb10Δ2-4:Insr* DKO ($p<0.05$) embryos were both significantly larger than *Insr* KO embryos but not different from each other.

In the case of placental weights, wild type (0.0899±0.0024g) and *Insr* KO (0.0915±0.0040g) differed by only 2% while *Grb10Δ2-4* KO (0.1162±0.0026g) and DKO (0.1028±0.0051g) were 29% and 14% larger than wild type, respectively (Fig. 6B). The only statistically significant size difference was between *Grb10Δ2-4* KO and either wild type ($p<0.0001$) or *Insr* KO placentae ($p<0.001$). When the ratio of embryo to placental mass was calculated as an estimate of placental efficiency, there were no significant differences between genotypes (Fig. 6C), though *Grb10* KO (11.35) and DKO (12.0) were slightly higher than wild type (10.55), and *Insr* KO (9.09) slightly lower. Two-way ANOVA found no evidence of

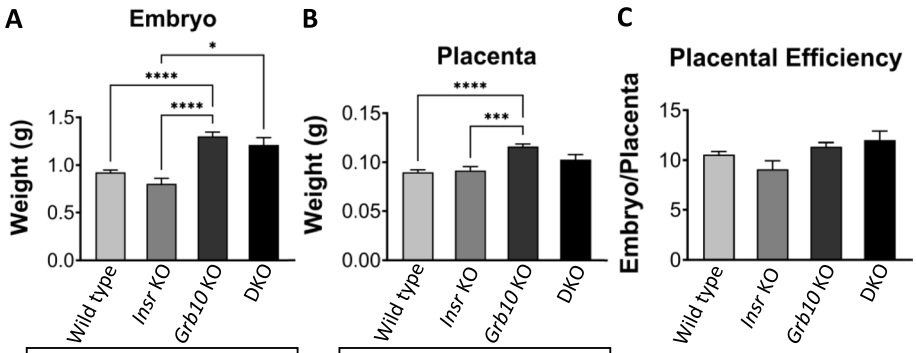

Source	%var	p value
Grb10	11.69	**0.0028**
Igf1r	32.39	**<0.0001**
Inter.	1.1197	0.739

Source	%var	p value
Grb10	11.79	**0.0028**
Igf1r	33.9	**<0.0001**
Inter.	1.189	0.739

Fig. 6 Weight analysis of e17.5 conceptuses from crosses between *Grb10Δ2-4* KO and *Insr* KO mice. Data were pooled into four groups for analysis as described in the Methods, wild type, *Insr* KO, *Grb10* KO and *Grb10*:*Insr* double knockouts (DKO). Weights are shown for the four offspring genotype groups for embryo (**A**) and placenta (**B**) and these have been used to calculate the embryo:placenta weight ratio as a measure of placental efficiency (**C**). Values represent means and SEM, tested by one-way ANOVA using Kruskal-Wallis and Dunn's post hoc statistical tests. Summaries of Two-way ANOVA outcomes beneath each graph show the percentage of total variation (%var) and a p value (values significant at $p<0.05$ in bold) for each source, namely the two single KO genotypes and any interaction (Inter.) between the two. Sample sizes were, for wild type (WT) $n=51$, *Insr* KO $n=13$, *Grb10* KO $n=52$, *Grb10*:*Insr* DKO $n=8$. Asterisks indicate *p*-values, *$p<0.05$, ***$p<0.001$, ****$p<0.0001$

an interaction between the genotypes for either embryo (Fig. 6A) or placenta (Fig. 6B) weight.

Survival of Grb10Δ2-4 KO x Insr KO progeny at PN1 and e17.5

Data from the *Grb10Δ2-4* KO x *Insr* KO cross was subject to Chi-squared statistical testing. This indicated that offspring genotype ratios were not significantly different from expected Mendelian ratios at either PN1 ($n=101$) or e17.5 ($n=124$) (Additional file 2: Table S2), even though pups lacking *Insr* expression are destined to die within a few days post-parturition of diabetic ketoacidosis [43, 45, 50]. To establish if this was also likely to be true for *Grb10Δ2-4*:*Insr* DKO animals we measured blood glucose levels during dissection of pups on PN1 (Fig. 7). Mean glucose concentrations were relatively low and indistinguishable between wild type (2.9mM±0.1) and *Grb10Δ2-4*KO (2.8mM±0.2) animals. Mean glucose levels were also indistinguishable between *Insr* KO (9.1mM±2.5) and *Grb10Δ2-4*:*Insr* DKO (6.4mM±1.7) animals and were significantly higher than wild type ($p<0.05$ for both comparisons) and *Grb10Δ2-4*KO ($p<0.01$ for both comparisons) pups, indicating incipient ketoacidosis in both types of animals lacking *Insr* expression.

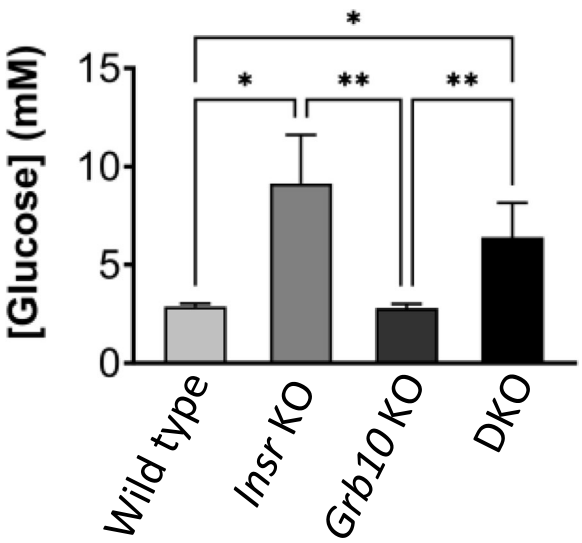

Fig. 7 Blood glucose levels of PN1 progeny from crosses between *Grb10Δ2-4* KO and *Insr* KO mice. Glucose concentration (mM) is shown for progeny of the four genotype groups wild type, *Insr* KO, *Grb10* KO and *Grb10*:*Insr* double knockouts (DKO). Values represent means and SEM, tested by one-way ANOVA using Kruskal-Wallis and Dunn's post hoc statistical tests. Sample sizes were, for wild type (WT) $n=40$, *Insr* KO $n=6$, *Grb10* KO $n=37$, *Grb10*:*Insr* DKO $n=6$. Asterisks indicate *p*-values, *$p<0.05$, **$p<0.01$

Litter size had relatively little impact on pup weight

An inverse correlation between birth weight and litter size has long been established [51]. To assess whether litter size might affect our results we plotted mean PN1 pup weights against litter size for each genotype of offspring from this, the largest dataset for which such data was available (total $n = 159$ pups from 33 litters (Additional file 1: Fig. S4). The tendency for pups from larger litters to be smaller than those from smaller litters

is clearly evident, at least for wild type, *Grb10Δ2-4* KO and *Grb10Δ2-4:Igf1r* DKO pups. A two-way ANOVA test showed litter size to be responsible for 8% ($p<0.0001$) of the variation while genotype was responsible for 59% ($p<0.0001$) of the variation, making it unlikely that litter size variation has contributed substantially to comparisons of pup birth weight by genotype.

Discussion

Using a mouse genetic approach we found no evidence that the Grb10 signalling adaptor protein negatively regulates fetal growth through interaction with either Igf1r or Insr. Growth regulation by Grb10 inhibiting the Igf1r, in particular, has become the prevailing view because of evidence that Grb10 can physically interact with both receptors [14, 15, 21] and can modulate their activity and downstream signalling including *in vivo*, at least in adult mouse tissues [19, 32, 38]. Should an interaction between Grb10 and Insr or Igf1r be responsible for regulation of fetal growth the clear prediction is that mice lacking both Grb10 and either receptor gene will be small at birth to the same extent as the homozygous receptor KO alone, reportedly 60% for *Igf1r* [41] or 90% for *Insr* [43] relative to wild type (Fig. 1B). This is because Grb10 will have no influence in the absence of the cognate receptor. However, in crosses between *Grb10* KO and *Igf1r* KO or *Insr* KO mice this was not what we observed and instead the influence of *Grb10* on growth was clearly present in the double knockout offspring both at the level of the whole body, individual organs, and even the gross morphology of *Grb10Δ2-4:Igf1r* DKO neonates. This conclusion was strongly supported by two-way ANOVA analysis of body and organ weight data. Across the five datasets presented, evidence of an interaction between the genotypes for body or organ weight was found in only two cases. First, there was evidence of a weak interaction between *Grb10Δ2-4* and *Igf1r* for PN1 body weight ($p=0.0106$), that was out of line with the four other datasets including that involving the same cross analysed at e17.5. The other exception was more interesting, for PN1 liver weight among offspring of the *Grb10Δ2-4* KO x *Insr* KO, supporting an interaction that explains the disproportionate weight of *Grb10Δ2-4* KO liver through Insr-dependent lipid storage.

Litter size has long been known to inversely correlate with mean pup birth weight, both for different mouse strains of wild type animals [51, 52] and for at least one growth deficient strain (*anemic dwarf*) [53]. To assess the potential impact of litter size we plotted it against mean PN1 pup weight for *Grb10Δ2-4* KO x *Igf1r* KO PN1 data, where the largest amount of litter size information was available. The expected decline in birth weight as litter size increased was clearly seen for wild type, *Grb10Δ2-4* KO and *Grb10Δ2-4:Igf1r* DKO pups. In the case of *Igf1r* KO pups only three PN1 animals were captured in the analysis and these were each from litters of different sizes. These three did not obviously follow the inverse correlation, but whether this was because of the small number or extreme growth deficiency of Igf1r KO pups, is unclear.

In crosses involving the *Igf1r* KO strain and either the *Grb10ins7* or *Grb10Δ2-4* KO strains, the birth weight of DKO pups was closer to that of wild type than either the small *Igf1r* KO or large *Grb10* KO pups. Also, the rate of perinatal lethality and cannibalisation of these DKO mice was much reduced in comparison with that for *Igf1r* KO pups, perhaps reflecting the attainment of an overall size sufficient for a critical function, such as temperature regulation, or the functional rescue of one or more vital organs. Previously, evidence was presented indicating that failure of the *Igf1r* KO lungs to inflate caused death by asphyxia [42] and in support of this we found the *Igf1r* KO lungs to be disproportionately small at 79-80% lighter than wild type, whereas *Grb10:Igf1r* DKO lungs were only some 16-26% smaller than wild type and only marginally disproportionate with body size. Due to ethical permissions in place when the work was conducted all offspring from crosses generating DKO pups were culled on PN1 at latest, consequently we do not know if *Grb10:Igf1r* DKO pups would have survived beyond the perinatal period.

In contrast to lungs, the heart from *Grb10ins7* KO ($p<0.05$) and *Igf1* KO ($p<0.05$) single mutants were disproportionately large, whereas the *Grb10ins7:Igf1r* DKO heart was not (Fig. 2J). The dopa decarboxylase gene (*Ddc*), neighbouring *Grb10*, also has a role in promoting growth of the developing heart and is expressed in the developing myocardium, specifically, using a paternally expressed transcript, *Ddc_exon1a* [54]. Despite sharing the imprinting control regions within *Grb10* [55, 56], *Ddc_exon1* and *Grb10* may be expressed in distinct cell populations through the use of separate tissue-specific enhancers [54]. Thus, while the dosage of the two genes is coordinated through genomic imprinting it is not clear whether they regulate fetal heart growth through a shared molecular mechanism.

Relative sparing of brain and kidney, seen here in all three crosses involving the *Igf1r* KO or *Insr* KO mice, has been seen in previous crosses involving the *Grb10Δ2-4* KO [25, 26] and *Grb10ins7* [24] strains. Brian sparing is in keeping with very limited expression of the maternal *Grb10* allele in the developing CNS [24, 25]. This lack of *Grb10* expression means the result could be considered uninformative. However, the paternal *Grb10* allele is strongly expressed in the developing central nervous system and its knockout also has no significant effect on

PN1 brain size [24–26], indirectly supporting the idea that Grb10 does not interact with Igf1r to limit fetal brain growth. In developing kidney, maternal *Grb10* is widely expressed, being lower in the mesenchyme andstrongest in the epithelial component as judged at the level of both mRNA and protein [25]. Since kidney growth is driven primarily by expansion of the metanephric mesoderm to fuel nephrogenesis [57], this expression pattern may explain the relatively limited effect of *Grb10* KO on fetal kidney growth. In support of a predominantly epithelial role, human *GRB10* has been shown to be a tumour suppressor in clear cell renal cell carcinoma, a prevalent epithelial kidney cancer [58].

Liver followed an interesting pattern of growth changes across the three crosses. In progeny of crosses between either of the two *Grb10* KO strains and the *Igf1r* KO strain, *Igf1r* KO liver was reduced in size, albeit to a slightly lesser extent than the body. In contrast, *Grb10* KO livers were disproportionately enlarged, as previously observed [24–26], and *Grb10:Igf1r* DKO livers were disproportionately enlarged, to a similar extent. Thus, loss of *Grb10* expression dominated the DKO phenotype, confirming that Grb10 regulates fetal liver size independently of Igfr1. The *Grb10Δ2-4* KO x *Insr* KO cross provided further information. While *Insr* KO offspring had livers of normal size and *Grb10Δ2-4* KO livers were again disproportionately enlarged, those of *Grb10Δ2-4:Insr* DKO offspring were indistinguishable in size from wild type and *Insr* KO livers. Liver histology revealed that excess lipid accumulation, associated with grossly distended hepatocytes, seen in *Grb10Δ2-4* KO liver was not seen in *Grb10Δ2-4:Insr* DKO liver. Instead, *Grb10Δ2-4:Insr* DKO hepatocyte histology was indistinguishable from that of *Insr* KO liver, which had a distinct degenerate fatty appearance, as previously reported [45, 50]. This indicates that during gestation Grb10 normally acts on the Insr to suppresses hepatic lipid storage, perhaps to maximise availability of energy for growth. The result demonstrates for the first time a physiological interaction between Grb10 and the Insr other than in adult tissues [32, 33, 38, 39] . An increase in cell number, mediated by a different tyrosine kinase receptor, as in other tissues, cannot be excluded in the *Grb10* KO liver but is potentially masked by the Insr-mediated hypertrophic expansion of hepatocytes. Interestingly, transgenic restoration of *Insr* expression in liver is sufficient to partially rescue the *Insr* KO phenotype [59–61] supporting that liver failure is a major contributor to *Insr* KO perinatal lethality. This relates to the vital role of liver-derived ketones as an energy source as pups transition from a placental nutrient supply (high in carbohydrates and low in free fatty acids) to post-natal life, to milk (high-fat and low-carbohydrate) and the need for *Insr* signalling to suppress gluconeogenesis and promote glycogen storage [62]. The lack of a catastrophic metabolic phenotype pre-term may be due to a combination of redundancy between Insr and Igf1r, supported by experiments showing that insulin can stimulate glucose uptake via Igf1r in *Insr* KO cells [63] , and the reliance of the fetus on placental exchange of nutrients and waste products.

Hepatic *Grb10* expression is gradually lost over the first 2-3 weeks after birth and with it the excess weight and lipid accumulation in *Grb10* KO liver [26]. Differentiated adipocytes capable of lipid storage emerge relatively late in development, either in late fetal development (subcutaneous white adipose tissue (WAT)) or in the early post-natal period (gonadal WAT) [64]. Interscapular brown adipose tissue is in place at birth and is important for non-shivering thermogenesis. The transition to energy storage in WAT and utilisation in brown adipose tissue (BAT) during the early post-natal period perhaps obviates the need for *Grb10* to suppress hepatic lipid storage and fits with the idea that imprinted genes are important for the transition from maternal dependence to independence [65]. Curiously, in different models of hepatic steatosis *Grb10* expression is induced, including through exposure to cadmium during gestational development [66] or post-natal exposure to tunicamycin or a high fat diet [67]. A liver-specific *Grb10* KO model was used to prove this expression was necessary for steatosis to occur [67]. This indicates a switch in the role of *Grb10* from inhibiting to facilitating hepatic lipid accumulation between fetal and adult life. Using tunicamycin to induce ER stress-mediated steatosis, Luo *et al*., (2018) [67] showed that loss of *Grb10* had little effect on insulin-stimulated AKT phosphorylation but significantly down regulated levels of proteins involved in fatty acid synthesis. This suggests involvement of a non-canonical insulin signalling mechanism, in contrast to what we report here in neonatal liver. Steatosis can begin in the fetal or neonatal liver [68] and is recognised as an early indicator of non-alcoholic fatty liver disease, the most prevalent liver disease worldwide [69]. Given the evidence from mouse studies, involvement of *GRB10* in steatosis and NAFLD merits further investigation.

In crosses involving either receptor KO and *Grb10Δ2-4* KO we evaluated embryo and placental weights at a single late gestational time-point, e17.5, when placental size is maximal. Compared to wild type, we have previously shown that *Grb10Δ2-4* KO conceptuses had a significant difference in mass, evident in the fetus from e12.5 and in the placenta from e14.5 [25]. Also, in a study of wild type litters, *Grb10* expression was found to be higher in the smallest placentae, relative to the largest [70]. Overgrowth of the *Grb10* KO placenta was found to be disproportionate, with greater expansion of the labyrinthine

exchange tissue relative to the marginal and junctional zones [49]. This was associated with increased placental efficiency, such that more fetal mass was supported per gram of placental tissue by the *Grb10* KO, likely due to the expanded labyrinthine zone allowing increased nutrient transfer from mother to offspring. Previous studies have concluded that there is no significant difference from wild type in the mass of placentae from *Igf1r* KO, *Insr* KO or even *Igf1r*:*Insr* DKO conceptuses [41, 43]. Our data are consistent with this, and favour the interpretation that Grb10 controls growth independently of Igf1r in the placenta as well as the embryo.

Insr KO progeny from our crosses did not display a significant growth deficit, in terms of whole-body mass at PN1 (-6%) or e17.5 (-13%), or in the mass of any individual PN1 organs. This at first appears to contrast with a reported 10% growth deficiency in e18.5 *Insr* KO progeny of an *Insr* KO x *Igf1r* KO cross [43], where the numbers of embryos weighed (n = 121, including 9 $Insr^{-/-}$) were very similar to our PN1 sample size (n = 101, including 6 $Insr^{-/-}$). However, it should be noted that the previous report [43] used a student's t test without any correction for multiple testing to find a significant difference in body weight between the genotypes at $p<0.05$. That said, the fact that *Insr* KO pups were consistently smaller by 6-13% across 3 different crosses and two separate studies, suggests the impact of *Insr* KO on fetal growth could be biologically relevant. Indeed, it seems feasible to assume that disruption in energy regulation should impact fetal growth and perhaps surprising that such an effect is not more obvious. In part, this can be explained by mouse genetic experiments showing there is redundancy in Ins/IGF signalling and, particularly, whereas Igf1 promotes growth exclusively through Igf1r, Igf2 uses both Igf1r and Insr [6, 42, 43]. Interestingly, mice with 80-98% mosaic *Insr* inactivation are normal in size at birth and survive for a few months but display severe post-natal growth restriction, a complete absence of mature adipocytes in BAT and WAT, and are hypoglycaemic [71]. This phenotype resembles Donohue syndrome (formerly leprechaunism), caused by homozygous *INSR* disruptions (reviewed in [72]).

The lack of a clear growth deficit associated with *Insr* KO did not affect the interpretation of our data since the well characterised overgrowth of *Grb10* KO pups was still evident in *Grb10Δ2-4*:*Insr* DKO pups, ruling out Insr as a major receptor through which Grb10 mediates fetal growth regulation. This was evident through examination of individual organ weights as well as whole body weights. Most straightforwardly, lungs and heart were enlarged to a similar extent in *Grb10Δ2-4* KO and *Grb10Δ2-4*:*Insr* DKO pups and differed from both wild type and *Insr* KO organs, though not always significantly. In this cross, *Grb10Δ2-4* KO brain and kidneys again exhibited sparing from the general overgrowth of the body, which meant there were only small weight differences across the genotypes for these organs, though both *Grb10Δ2-4* KO and *Grb10Δ2-4*:*Insr* DKO brain and kidneys were disproportionately small relative to the whole-body overgrowth exhibited by pups of these genotypes. At PN1 there was no obvious deficit in the number of *Insr* KO or *Grb10Δ2-4*:*Insr* DKO pups but both had significantly elevated blood glucose levels, indicative of incipient ketoacidosis, as previously observed for *Insr* KO neonates [45, 50]. In summary, the *Grb10Δ2-4* KO x *Insr* KO cross data has established that increased fetal growth associated with loss of maternal *Grb10* expression is not mediated through interaction with the *Insr*. Any impact of the *Insr* alone on fetal growth regulation is modest and instead it is primarily or solely a regulator of glucose homeostasis, including lipid storage in the fetal liver, which we have shown is normally inhibited by *Grb10*. The effects of *Grb10* KO on liver at the cellular and molecular level merit further investigation.

As well as optimising body size during fetal growth, the growth of individual tissues and organs must be coordinated to achieve a size compatible with efficient function. Tissue proportions can be influenced by the environment. For instance, when nutrient supply is limited during development proportions can be altered in order to preserve brain growth over other organs in animals ranging from *Drosophila* to human (see [73]) which has been termed brain sparing. By limiting growth in only peripheral tissues *Grb10* could, therefore, be an important determinant of brain sparing. More generally, our work shows how body proportions, as well as size, is altered through the actions of two independent growth regulatory pathways. Although we have not identified the 'growth' receptor, or receptors, on which Grb10 acts, the findings allow us to make some important inferences. In at least two pathways growth and energy homeostasis are intimately linked through Insr and mTOR signalling. While it was initially anticipated that *Grb10* would prove to be the third imprinted gene influencing the Ins/IGF signalling pathway, we have shown instead that imprinting has evolved to influence more than one growth regulatory pathway. Theories for the evolution of imprinting, including the conflict hypothesis, tend to focus on individual genes rather than pathways. It is generally agreed that the benefits of voluntarily shutting down one of the two parental alleles must outweigh the cost, most obviously the risk of losing the one active copy but also, once adapted to the single gene dose, the risk of the silent copy becoming active. These risks may explain why more genes are not subject to imprinting within a single pathway, with the consequences of the resulting imbalances

amply illustrated by imprinting disorders such as BWS and SRS [12].

Our data highlight that the coordination of organ size regulation during fetal development can be disrupted through maternal *Grb10* KO in a manner that is not apparent through disruption of *Igf1r* expression. In *Igf1r* KO PN1 pups, organs derived primarily from each of the three germs layers, ectoderm (brain), mesoderm (heart, kidneys) and endoderm (liver, lungs) were all reduced in size. This is consistent with Igf1r, which mediates signalling of Igf1 and Igf2 [41, 42], impacting growth during early embryogenesis. A study of *Igf2* KO embryos supports this, finding that disruption of cell proliferation and survival in a narrow window between e9-e10, resulted in significant changes in cell number, detectable from e11 [74], which is a few days earlier than a difference in mass can be properly discerned [25, 41, 74]. This window coincides with the early post gastrulation period when there is rapid expansion of the three germ layers and the initial events in organogenesis are taking place. We predict that by acting within a similar developmental window and engaging with one or more different receptors, Grb10 influences growth of a more limited set of tissue lineages. One possibility is that Grb10 acts on lineage-specific progenitors as they emerge during early organogenesis, since their expansion is known to regulate organ size as demonstrated, for instance, by genetic ablation experiments (e.g. [75]). Further work will be needed to identify the receptor(s) with which Grb10 interacts to influence fetal growth. Interactions between Grb10 and RTKs have been established using various techniques, most often involving co-immunoprecipitation of native or overexpressed protein in cultured cells (reviewed [14–16]). Since biological outcomes from these interactions may be cell type- and context-dependent the identification of the physiological growth receptor(s) may require the use of fetal tissue for the testing of candidates or application of an unbiased proteomics screen.

Conclusions

Our epistatic tests involving *Igf1r* KO mice show that the fetal overgrowth phenotype of *Grb10* KO mice is not mediated primarily through Grb10 interaction with the Igf1r, contrary to expectation within the field. While we cannot rule out minor involvement of Igf1r, the major effect on fetal growth must involve one or more separate receptors. Similarly, we were unable to detect any growth effect of Grb10 mediated by the Insr, except for the disproportionate overgrowth of the liver. This liver expansion was associated with Insr-mediated accumulation of excess lipid in hepatocytes, indicating a metabolic basis consistent with the known role for Grb10 as an inhibitor of Insr signalling in adult tissues. Fundamental understanding of fetal growth regulation has potential benefits for the development of novel interventions that improve neonatal outcomes and life-long health for the wider population, including those with rare growth disorders.

Methods

Mice

Generation of the mouse strains *Grb10Δ2-4* (full designation $Grb10^{Gt(\beta\text{-}geo)1Ward}$) and *Grb10ins7* (previously referred to as *Grb10* KO; full designation $Grb10^{Gt(\beta\text{-}geo)2Ward}$) from gene-trap embryonic stem cell lines has previously been described [24, 25]. Both lines are predicted null alleles and contain a functional *LacZ* reporter gene insertion expressed under the control of endogenous *Grb10* regulatory elements. Detailed characterisation has shown that in *Grb10Δ2-4* the *LacZ* reporter gene has replaced some 36kb of endogenous sequence, including the first 3 protein coding exons (exons 2-4), while the *Grb10ins7* insertion site is associated with a 12bp deletion at the 3' end of exon 7 [44]. Null alleles have also been described for the *Insr* KO [45] and *Igf1r* KO [46] strains. To generate experimental animals, first $Grb10\Delta2\text{-}4^{+/p}$ and $Grb10ins7^{+/p}$ males were each crossed with $Igf1r^{+/-}$ females to generate double heterozygous animals, $Grb10\Delta2\text{-}4^{+/p}$: $Igf1r^{+/-}$ and $Grb10ins7^{+/p}$: $Igf1r^{+/-}$. Double heterozygous females were then crossed with $Grb10^{+/+}$:$Igf1r^{+/-}$ males to produce offspring of six genotypes (Table 2A). Mice were genotyped by PCR using primers and conditions previously described for *Grb10* [44] and *Igf1r* [46].

$Grb10\Delta2\text{-}4^{+/p}$ males were also crossed with $Insr^{+/-}$ females to generate double heterozygous animals, $Grb10\Delta2\text{-}4^{+/p}$: $Insr^{+/-}$. These double heterozygous females were intercrossed to produce offspring of 12 genotypes (Table 2B). In addition to using PCR to genotype offspring for wild type and mutant *Grb10Δ2-4* [44] and *Insr* [43] alleles, carcasses were *LacZ* stained [24] to determine the parental origin of mutant *Grb10* alleles. Embryos and placentae were collected on embryonic day e17.5, where e0.5 was the day on which a copulation plug was observed. Otherwise, experimental animals were collected on the day of birth, designated post-natal day 1 (PN1). Wild type littermates are considered the control group and single animals the biological replicate, noting that multiple litters were generated in each cross, with the aim of having enough of the least common genotypes for robust statistical analysis. Experimental offspring were derived solely from previously nulliparous dams since we have shown previously that first and second litters from the same dam are non-equivalent [47]. All animals were maintained on a mixed inbred (C57BL/6J:CBA/Ca) strain background and housed under conditions of 13 hours

light:11 hours darkness, including 30-minute periods of dim lighting to provide false dawn and dusk, a temperature of 21±2°C and relative humidity of 55±10%. Standard chow (CRM formula; Special Diets Services, Witham, Essex, UK) and water was freely available.

Tissue collection, histology and blood glucose measurements

Whole bodies and organs were collected, any surface fluid removed from embryos or dissected organs by gently touching them onto absorbent paper, and weights obtained using a fine balance accurate to 4 decimal places (Sartorius BP61S). Paired organs (lungs and kidneys) were weighed together. Organs for histology were fixed by immersion in 4% (w/v) paraformaldehyde in PBS at 4°C for 16-24 hours, then processed by machine (Leica TP1020) for wax embedding. Sections were cut at approximately 8-10 µm using a microtome (Leica Histocore Biocut), prior to staining with haematoxylin and eosin as previously described [48]. Images were collected using a digital colour camera (Olympus SC50) and software (Olympus cellSens Entry), attached to a compound microscope (Nikon Eclipse E800), then scored with the operator blind to genotype. Glucose measurements were obtained using a One-Touch ULTRA (Lifescan, CA) glucometer immediately following collection of whole blood by decapitation of PN1 pups.

Statistical analysis

Chi-square tests were applied to determine whether the genotypes of experimental groups were present in the expected Mendelian ratios. Otherwise, numerical data were subject to one-way analysis of variance (ANOVA), using a Kruskall-Wallis test with post-hoc Dunn's test to determine *p*-values between groups. This test allowed us to detect significant differences associated with either of the single knockout groups in each set of progeny as well as any significant interaction between them. This relatively conservative non-parametric test was chosen because in some experiments one or more genotype group was represented by a small samples size (n=<5). In order to test for an interaction between mutant genotypes we also applied a two-way ANOVA test where indicated. All statistical tests were applied using GraphPad Prism (v10 GraphPad, La Jolla, CA, USA) software. Graphs show arithmetic means ±standard error of the mean (SEM). Differences with *p*-values of <0.05 were considered statistically significant.

Abbreviations

BAT	Brown adipose tissue
BWS	Beckwith-Wiedemann Syndrome
CNS	Central nervous system
DKO	Double knock-out
Grb10	Growth factor receptor bound protein 10
Grb10$^{m/+}$	Heterozygous deletion of the maternal allele of the *Grb10* gene
Grb10$^{+/p}$	Heterozygous deletion of the paternal allele of the *Grb10* gene
Igf1r	Insulin-like growth factor 1 receptor
Ins/IGF	Insulin/insulin-like growth factor
Insr	Insulin receptor
KO	Knock-out
mTOR	Mammalian target of rapamycin
RTK	Receptor tyrosine kinase
SRS	Silver-Russell Syndrome
SEM	Standard error of the mean
WAT	White adipose tissue
WT	Wild type

Supplementary Information

The online version contains supplementary material available at https://doi.org/10.1186/s12915-024-01926-w.

Additional file 1: Figures S1-S4. Fig. S1. Weights at PN1 from progeny of crosses between *Grb10ins7* KO and *Igf1r* KO mice. Body weights are shown for the six offspring genotypes (A). Actual weights of brain (B), liver (C), lungs (D), heart (E) and kidneys (F) are shown alongside relative weights of the same organs, expressed as a percentage of body mass (G-K). Values represent means and SEM, tested using ANOVA with Kruskal-Wallis post hoc statistical tests. Sample sizes were, for body, *Grb10* wild type (WT):*Igf1r* WT n=15, *Grb10* WT:*Igf1r* Het n=23, *Grb10* KO:*Igf1r* WT n=8, *Grb10* KO:*Igf1r* Het n=18, *Grb10* WT:*Igf1r* KO n=7, *Grb10*:*Igf1r* DKO n=12; brain, *Grb10* WT:*Igf1r* WT n=15, *Grb10* WT:*Igf1r* Het n=23, *Grb10* KO:*Igf1r* WT n=8, *Grb10* KO:*Igf1r* Het n=17, *Grb10* WT:*Igf1r* KO n=3, *Grb10*:*Igf1r* DKO n=8 liver, *Grb10* WT:*Igf1r* WT n=15, *Grb10* WT:*Igf1r* Het n=23, *Grb10* KO:*Igf1r* WT n=8, *Grb10* KO:*Igf1r* Het n=17, *Grb10* WT:*Igf1r* KO n=2, *Grb10*:*Igf1r* DKO n=7; lungs, *Grb10* WT:*Igf1r* WT n=15, *Grb10* WT:*Igf1r* Het n=23, *Grb10* KO:*Igf1r* WT n=8, *Grb10* KO:*Igf1r* Het n=17, *Grb10* WT:*Igf1r* KO n=1, *Grb10*:*Igf1r* DKO n=7; heart, *Grb10* WT:*Igf1r* WT n=14, *Grb10* WT:*Igf1r* Het n=23, *Grb10* KO:*Igf1r* WT n=8, *Grb10* KO:*Igf1r* Het n=17, *Grb10* WT:*Igf1r* KO n=2, *Grb10*:*Igf1r* DKO n=7; kidneys, *Grb10* WT:*Igf1r* WT n=15, *Grb10* WT:*Igf1r* Het n=23, *Grb10* KO:*Igf1r* WT n=8, *Grb10* KO:*Igf1r* Het n=17, *Grb10* WT:*Igf1r* KO n=2, *Grb10*:*Igf1r* DKO n=7. Asterisks indicate *p*-values, * p <0.05, ** p <0.01, *** p <0.001, **** p<0.0001. Fig. S2. Weights at PN1 from progeny of crosses between *Grb10Δ2-4* KO and *Igf1r* KO mice. Body weights are shown for the six offspring genotypes (A). Actual weights of brain (B), liver (C), lungs (D), heart (E) and kidneys (F) are shown alongside relative weights of the same organs, expressed as a percentage of body mass (G-K). Values represent means and SEM, tested using ANOVA with Kruskal-Wallis post hoc statistical tests. Sample sizes were, for body, *Grb10* WT:*Igf1r* WT n=35, *Grb10* WT:*Igf1r* Het n=69, *Grb10* KO:*Igf1r* WT n=25, *Grb10* KO:*Igf1r* Het n=67, *Grb10* WT:*Igf1r* KO n=13, *Grb10*:*Igf1r* DKO n=28; brain, *Grb10* WT:*Igf1r* WT n=35, *Grb10* WT:*Igf1r* Het n=67, *Grb10* KO:*Igf1r* WT n=25, *Grb10* KO:*Igf1r* Het n=65, *Grb10* WT:*Igf1r* KO n=6, *Grb10*:*Igf1r* DKO n=24 liver, *Grb10* WT:*Igf1r* WT n=35, *Grb10* WT:*Igf1r* Het n=69, *Grb10* KO:*Igf1r* WT n=25, *Grb10* KO:*Igf1r* Het n=65, *Grb10* WT:*Igf1r* KO n=5, *Grb10*:*Igf1r* DKO n=23; lungs, *Grb10* WT:*Igf1r* WT n=35, *Grb10* WT:*Igf1r* Het n=69, *Grb10* KO:*Igf1r* WT n=25, *Grb10* KO:*Igf1r* Het n=65, *Grb10* WT:*Igf1r* KO n=4, *Grb10*:*Igf1r* DKO n=23; heart , *Grb10* WT:*Igf1r* WT n=34, *Grb10* WT:*Igf1r* Het n=69, *Grb10* KO:*Igf1r* WT n=24, *Grb10* KO:*Igf1r* Het n=64, *Grb10* WT:*Igf1r* KO n=5, *Grb10*:*Igf1r* DKO n=23; kidneys, *Grb10* WT:*Igf1r* WT n=34, *Grb10* WT:*Igf1r* Het n=66, *Grb10* KO:*Igf1r* WT n=25, *Grb10* KO:*Igf1r* Het n=65, *Grb10* WT:*Igf1r* KO n=5 *Grb10*:*Igf1r* DKO n=23. Asterisks indicate *p*-values, * p <0.05, ** p <0.01, *** p <0.001, **** p<0.0001. Fig S3. Weights PN1 from progeny of crosses between *Grb10Δ2-4* KO and *Insr* KO mice. Body weights are shown for the six offspring genotypes (A). Actual weights of brain (B), liver (C), lungs (D), heart (E) and kidneys (F) are shown alongside relative weights of the same organs, expressed as a percentage of body mass (G-K). Values represent means and SEM, tested using ANOVA with Kruskal-Wallis post hoc statistical tests. Sample sizes were, for body, *Grb10* WT:*Insr* WT n=13, *Grb10* WT:*Insr* Het n=29, *Grb10* KO:*Insr* WT n=18, *Grb10* KO:*Insr* Het n=26, *Grb10* WT:*Insr* KO n=6, *Grb10*:*Insr* DKO n=9; brain, *Grb10* WT:*Insr* WT n=13, *Grb10* WT:*Insr* Het n=29, *Grb10* KO:*Insr* WT n=18, *Grb10*

KO:*Insr* Het *n*=26, *Grb10* WT:*Insr* KO *n*=6, *Grb10*:*Insr* DKO *n*=9; liver, *Grb10* WT:*Insr* WT *n*=13, *Grb10* WT:*Insr* Het *n*=29, *Grb10* KO:*Insr* WT *n*=18, *Grb10* KO:*Insr* Het *n*=26, *Grb10* WT:*Insr* KO *n*=6, *Grb10*:*Insr* DKO *n*=9; lungs, *Grb10* WT:*Insr* WT *n*=13, *Grb10* WT:*Insr* Het *n*=29, *Grb10* KO:*Insr* WT *n*=18, *Grb10* KO:*Insr* Het *n*=26, *Grb10* WT:*Insr* KO *n*=6, *Grb10*:*Insr* DKO *n*=9; heart , *Grb10* WT:*Insr* WT *n*=13, *Grb10* WT:*Insr* Het *n*=29, *Grb10* KO:*Insr* WT *n*=18, *Grb10* KO:*Insr* Het *n*=26, *Grb10* WT:*Insr* KO *n*=6, *Grb10*:*Insr* DKO *n*=9; kidneys, *Grb10* WT:*Insr* WT *n*=13, *Grb10* WT:*Insr* Het *n*=29, *Grb10* KO:*Insr* WT *n*=18, *Grb10* KO:*Insr* Het *n*=26, *Grb10* WT:*Insr* KO *n*=6, *Grb10*:*Insr* DKO *n*=9. Asterisks indicate *p*-values, * p <0.05, ** p <0.01, *** p <0.001, **** p<0.0001.
Fig. S4. Litter size and weight of pups from crosses between *Grb10Δ2-4* KO and *Igf1r* KO mice. A) Numbers of pups from different sized litters are shown according to genotype. B) Mean body weights (horizontal bars) for pups of each genotype are shown across the different litter sizes. Boxes show 25th to 75th percentiles and whiskers the range from minimum to maximum. The data are from 37 litters (mean size 4.8 pups) that contained 73 wild type, 3 *Igf1r* KO, 67 *Grb10* KO and 14 *Grb10*:*Igf1r* DKO pups.

Additional file 2: Tables S1-S3. Table S1. Chi-squared statistical tests of offspring survival from crosses involving *Grb10* KO and *Igf1r* KO strains. Offspring collected from crosses between *Grb10Δ2-4*$^{+/p}$: *Igfr1*$^{+/-}$ females and *Grb10Δ2-4*$^{+/+}$: *Igfr1*$^{+/-}$ males at, (A) PN1 and (B) e17.5. (C) Offspring collected at PN1 from crosses between *Grb10ins7*$^{+/p}$: *Igf1*$^{+/-}$ females and *Grb10ins7*$^{+/+}$: *Igf1*$^{+/-}$ males. Deviation from the expected Mendelian ratio was considered significant at p<0.05. PN1: *Grb10Δ2-4*$^{+/p}$: *Igf1r*$^{+/-}$ x *Grb10Δ2-4*$^{+/+}$: *Igf1r*$^{+/-}$ e17.5: *Grb10Δ2-4*$^{+/p}$: *Igf1r*$^{+/-}$ x *Grb10Δ2-4*$^{+/+}$: *Igf1r*$^{+/-}$. Table S2. Chi-squared statistical tests of offspring survival from crosses between the *Grb10 Δ2-4* KO and *Insr* KO strains. Offspring collected from crosses between *Grb10Δ2-4*$^{+/p}$: *Insr*$^{+/-}$ females and *Grb10Δ2-4*$^{+/p}$: *Insr*$^{+/-}$ males at PN1 (A) and at e17.5 (B). Deviation from the expected Mendelian ratio was considered significant at p<0.05. Table S3. Litter size information for progeny of mouse crosses involving *Grb10Δ2-4* and either *Igf1r* KO or *Insr* KO. The number of pups per litter is shown as a range and mean for each dataset.

Acknowledgements
For generously supplying mouse strains we thank Domenico Accili (*Insr* KO) and Martin Holzenberger (*Igf1r* KO). We are grateful to University of Bath Biological Services Unit staff for outstanding animal care and to Robert Clayton and Sandra Addis for technical help with histology.

Authors' contributions
AW conceived the project, collected and analysed data, wrote the manuscript and assembled the figures. FMS and ASG set up genetic crosses, collected data and contributed to data analysis. KM performed histological examination of the liver, carried out the statistical analyses and generated the final graphs and images. All authors read and approved the final manuscript.

Funding
This work was supported by Medical Research Council grants [MR/S00002X/1, MR/S008233/1]. The funder had no specific role in the conceptualization, design, data collection, analysis, decision to publish, or preparation of the manuscript.

Availability of data and materials
All data generated or analysed during this study are included in this published article and its supplementary information files.
Mouse strains *Grb10Δ2-4* (*Grb10*$^{Gt(β\text{-}geo)1Ward}$) and *Grb10ins7* (*Grb10*$^{Gt(β\text{-}geo)2Ward}$) were generated in our laboratory from gene trap embryonic stem cell lines, as previously described [24, 25] and can be obtained from us. The *Igf1r* KO (*B6.129-Igf1rtm1.2Mhz/Orl*) mouse [46] was obtained from Martin Holzenberger and is available from the European Mouse Mutant Archive (https://www.infrafrontier.eu/emma/). The *Insr* KO (*Insr*^{tm1Dac}) strain [45]was obtained from Domenico Accili and is available from the Jackson Laboratory repository (Jax.org).

Declarations

Ethics approval and consent to participate
Experiments involving mice were subject to local ethical review by the University of Bath Animal Welfare and Ethics Review Board (PPL-AW-141019) and carried out under licence from the United Kingdom Home Office (PPL PB56237E5). The manuscript has been written as closely as possible in accordance with the Animal Research: Reporting of In Vivo Experiments (ARRIVE) guidelines (https://arriveguidelines.org/).

Consent for publication
Not applicable.

Competing interests
The authors declare that they have no competing interests.

Received: 21 November 2023 Accepted: 22 May 2024
Published online: 30 May 2024

References

1. Wilcox AJ. On the importance-and the unimportance-of birthweight. Int J Epidemiol. 2001;30:1233–41.
2. Cousminer DL, Freathy RM. Genetics of early growth traits. Hum Mol Genet. 2020;29:R66-72.
3. Glastras SJ, Valvi D, Bansal A. Developmental programming of metabolic diseases. Front Endocrinol. 2021;12:781861.
4. Garofalo RS. Genetic analysis of insulin signaling in Drosophila. Trends Endocrinol Metab. 2002;13:156–62.
5. Oldham S, Hafen E. Insulin/IGF and target of rapamycin signaling: a TOR de force in growth control. Trends Cell Biol. 2003;13:79–85.
6. Efstratiadis A. Genetics of mouse growth. Int J Dev Biol. 1998;42:955–76.
7. Andergassen D, Dotter CP, Wenzel D, Sigl V, Bammer PC, Muckenhuber M, et al. Mapping the mouse Allelome reveals tissue-specific regulation of allelic expression. Elife. 2017;6:1–29.
8. Tucci V, Isles AR, Kelsey G, Ferguson-Smith AC, Bartolomei MS, Benvenisty N, et al. Genomic Imprinting and Physiological Processes in Mammals. Cell. 2019;176:952–65.
9. Haig D, Westoby M. Parent-specific gene expression and the triploid endosperm. Am Nat. 1998;134:147–55.
10. Moore T, Haig D. Genomic imprinting in mammalian development: a parental tug-of-war. Trends Genet. 1991;7:45–9.
11. Chang S, Bartolomei MS. Modeling human epigenetic disorders in mice: Beckwith-Wiedemann syndrome and Silver-Russell syndrome. Dis Model Mech. 2020;13:dmm044123.
12. Eggermann T, Davies JH, Tauber M, van den Akker E, Hokken-Koelega A, Johansson G, Netchine I. Growth restriction and genomic imprinting-overlapping phenotypes support the concept of an imprinting network. Genes. 2021;12:585.
13. Azzi S, Salem J, Thibaud N, Chantot-Bastaraud S, Lieber E, Netchine I, et al. A prospective study validating a clinical scoring system and demonstrating phenotypical-genotypical correlations in Silver-Russell syndrome. J Med Genet. 2015;52:446–53.
14. Holt LJ, Siddle K. Grb10 and Grb14: enigmatic regulators of insulin action-and more? Biochem J. 2005;388:393–406.
15. Kabir NN, Kazi JU. Grb10 is a dual regulator of receptor tyrosine kinase signaling. Molecular Biology Reports. 2014;41:1985–92.
16. Plasschaert RN, Bartolomei MS. Tissue-specific regulation and function of Grb10 during growth and neuronal commitment. Proc Natl Acad Sci U S A. 2015;112:6841–7.
17. Hsu PP, Kang SA, Rameseder J, Zhang Y, Ottina KA, Lim D, et al. The mTOR-regulated phosphoproteome reveals a mechanism of mTORC1-mediated inhibition of growth factor signaling. Science. 2011;332:1317–22.
18. Yu Y, Yoon SO, Poulogiannis G, Yang Q, Ma XM, Villén J, et al. Phosphoproteomic analysis identifies Grb10 as an mTORC1 substrate that negatively regulates insulin signaling. Science. 2011;332:1322–6.
19. Liu M, Bai J, He S, Villarreal R, Hu D, Zhang C, et al. Grb10 promotes lipolysis and thermogenesis by phosphorylation-dependent feedback inhibition of mTORC1. Cell Metab. 2014;19:967–80.
20. Liu H, He Y, Bai J, Zhang C, Zhang F, Yang Y, et al. Hypothalamic Grb10 enhances leptin signalling and promotes weight loss. Nat Metab. 2023;5:147–64.
21. Liu B, Liu F. Feedback regulation of mTORC1 by Grb10 in metabolism and beyond. Cell Cycle. 2014;13:2643–4.

22. Blagitko N, Mergenthaler S, Schulz U, Wollmann HA, Craigen W, Eggermann T, et al. Human GRB10 is imprinted and expressed from the paternal and maternal allele in a highly tissue-and isoform-specific fashion. Hum Mol Genet. 2000;9:1587–95.
23. Arnaud P, Monk D, Hitchins M, Gordon E, Dean W, Beechey CV, et al. Conserved methylation imprints in the human and mouse GRB10 genes with divergent allelic expression suggests differential reading of the same mark. Human Molecular Genetics. 2003;12:1005–19.
24. Garfield AS, Cowley M, Smith FM, Moorwood K, Stewart-Cox JE, Gilroy K, et al. Distinct physiological and behavioural functions for parental alleles of imprinted Grb10. Nature. 2011;469:534–40.
25. Charalambous M, Smith FM, Bennett WR, Crew TE, Mackenzie F, Ward A. Disruption of the imprinted Grb10 gene leads to disproportionate overgrowth by an Igf2-independent mechanism. Proc Natl Acad Sci U S A. 2003;100:8292–7.
26. Madon-Simon M, Cowley M, Garfield AS, Moorwood K, Bauer SR, Ward A. Antagonistic roles in fetal development and adult physiology for the oppositely imprinted Grb10 and Dlk1 genes. BMC Biol. 2014;12:99. https://doi.org/10.1186/s12915-014-0099-8.
27. Dent CL, Humby T, Lewis K, Ward A, Fischer-Colbrie R, Wilkinson LS, et al. Impulsive choice in mice lacking paternal expression of Grb10 suggests intragenomic conflict in behavior. Genetics. 2018;209:233–9.
28 Rienecker KDA, Chavasse AT, Moorwood K, Ward A, Isles AR. Detailed analysis of paternal knockout Grb10 mice suggests effects on stability of social behavior, rather than social dominance. Genes, Brain Behav. 2020;19(1):e12571.
29. Dent C, Reinecker KDA, Ward A, Wilkins JF, Humby T, Isles AR. Mice lacking paternal expression of imprinted Grb10 are risk takers. Genes Brain Behav. 2020;19:12679.
30. Mokbel N, Hoffman NJ, Girgis CM, Small L, Turner N, Daly RJ, et al. Grb10 Deletion Enhances Muscle Cell Proliferation, Differentiation and GLUT4 Plasma Membrane Translocation. J Cell Physiol. 2014;229:1753–64.
31. Holt LJ, Turner N, Mokbel N, Trefely S, Kanzleiter T, Kaplan W, et al. Grb10 regulates the development of fiber number in skeletal muscle. FASEB J. 2012;26:3658–69.
32. Smith FM, Holt LJ, Garfield AS, Charalambous M, Koumanov F, Perry M, et al. Mice with a Disruption of the Imprinted Grb10 Gene Exhibit Altered Body Composition, Glucose Homeostasis, and Insulin Signaling during Postnatal Life. Mol Cell Biol. 2007;27:5871–86.
33. Holt LJ, Lyons RJ, Ryan AS, Beale SM, Ward A, Cooney GJ, et al. Dual ablation of Grb10 and Grb14 in mice reveals their combined role in regulation of insulin signaling and glucose homeostasis. Mol Endocrinol. 2009;23:1406–14.
34. González-Renteria SM, Sosa-Macías M, Rodríguez-Moran M, Chairez-Hernández I, Lares-Aseff IA, Guerrero-Romero F, Galaviz-Hernández C. Association of the intronic polymorphism rs12540874 A>G of the GRB10 gene with high birth weight. Early Hum Dev. 2014;90(10):545–8. https://doi.org/10.1016/j.earlhumdev.2014.06.012.
35. Wang Y, Ding X, Tan Z, Xing K, Yang T, Pan Y, et al. Genome-wide association study for reproductive traits in a Large White pig population. Anim Genet. 2018;49:127–31.
36. Ghasemi M, Zamani P, Vatankhah M, Abdoli R. Genome-wide association study of birth weight in sheep. Animal. 2019;13:1797–803.
37. Rosing-Asvid A, Löytynoja A, Momigliano P, Hansen RG, Scharff-Olsen CH, Valtonen M, et al. An evolutionarily distinct ringed seal in the Ilulissat Icefjord. Mol Ecol. 2023;32:5932–43. https://doi.org/10.1111/mec.17163.
38. Wang L, Balas B, Christ-Roberts CY, Kim RY, Ramos FJ, Kikani CK, et al. Peripheral Disruption of the Grb10 Gene Enhances Insulin Signaling and Sensitivity In Vivo. Mol Cell Biol. 2007;27:6497–505.
39. Zhang J, Zhang N, Liu M, Li X, Zhou L, Huang W, et al. Disruption of growth factor receptor-binding protein 10 in the pancreas enhances β-cell proliferation and protects mice from streptozotocin-induced β-cell apoptosis. Diabetes. 2012;61:3189–98.
40 Prokopenko I, Poon W, Mägi R, Prasad BR, Salehi SA, Almgren P, et al. A central role for GRB10 in regulation of islet function in man. PLoS Genet. 2014;10(4):e1004235.
41. Baker J, Liu JP, Robertson EJ, Efstratiadis A. Role of insulin-like growth factors in embryonic and postnatal growth. Cell. 1993;75:73–82.
42. Liu JP, Baker J, Perkins AS, Robertson EJ, Efstratiadis A. Mice carrying null mutations of the genes encoding insulin-like growth factor I (Igf-1) and type 1 IGF receptor (Igf1r). Cell. 1993;75:59–72.
43. Louvi A, Accili D, Efstratiadis A. Growth-promoting interaction of IGF-II with the insulin receptor during mouse embryonic development. Dev Biol. 1997;189:33–48.
44. Cowley M, Garfield AS, Madon-Simon M, Charalambous M, Clarkson RW, Smalley MJ, et al. Developmental Programming Mediated by Complementary Roles of Imprinted Grb10 in Mother and Pup. PLoS Biol. 2014;12(2):e1001799.
45. Accili D, Drago J, Lee EJ, Johnson MD, Cool MH, Salvatore P, et al. Early neonatal death in mice homozygous for a null allele of the insulin receptor gene. Nat Genet. 1996;12:106–9.
46. Holzenberger M, Dupont J, Ducos B, Leneuve P, Geloen A, Even PC, et al. IGF-1 receptor regulates lifespan and resistance to oxidative stress in mice. Nature. 2003;421:182–7.
47. Charalambous M, Ward A, Hurst LD. Evidence for a priming effect on maternal resource allocation: Implications for interbrood competition. Proc R Soc B Biol Sci (Suppl). 2003;270:S100-3.
48. Bancroft JD, Gamble M. Theory and Practice of Histological Techniques. 5th ed. London: Churchill Livingstone; 2002.
49. Charalambous M, Cowley M, Geoghegan F, Smith FM, Radford EJ, Marlow BP, et al. Maternally-inherited Grb10 reduces placental size and efficiency. Dev Biol. 2010;337:1–8.
50. Joshi RL, Lamothe B, Cordonnier N, Mesbah K, Monthioux E, Jami J, et al. Targeted disruption of the insulin receptor gene in the mouse results in neonatal lethality. EMBO J. 1996;15:1542–7.
51. Crozier WJ, Enzmann EV. On the relationship between litter size, birth weight and rate of growth in mice. J Gen Physiol. 1935;19:249–63.
52 Mclaren A. Genetic and environmental effects on foetal and placental growth in mice. J Reprod Fertil. 1964;9:79–98.
53. Crozier WJ. On the relationship between birth weight and litter size in mice. J Gen Physiol. 1940;23:309–20.
54 Prickett AR, Montibus B, Barkas N, Amante SM, Franco MM, Cowley M, et al. Imprinted Gene Expression and Function of the Dopa Decarboxylase Gene in the Developing Heart. Front Cell Dev Biol. 2021;9:1–10.
55. Shiura H, Nakamura K, Hikichi T, Hino T, Oda K, Suzuki-Migishima R, et al. Paternal deletion of Meg1/Grb10 DMR causes maternalization of the Meg1/ Grb10 cluster in mouse proximal Chromosome 11 leading to severe pre- and postnatal growth retardation. Hum Mol Genet. 2009;18:1424–38.
56. Juan AM, Foong YH, Thorvaldsen JL, Lan Y, Leu NA, Rurik JG, et al. Tissue-specific Grb10/Ddc insulator drives allelic architecture for cardiac development. Mol Cell. 2022;82:3613-3631.e7.
57. Hartman HA, Lai HL, Patterson LT. Cessation of renal morphogenesis in mice. Dev Biol. 2007;310:379–87.
58. Creighton CJ, Morgan M, Gunaratne PH, Wheeler DA, Gibbs RA, Robertson G, et al. Comprehensive molecular characterization of clear cell renal cell carcinoma. Nature. 2013;499:43–9.
59. Baudry A, Jackerott M, Lamothe B, Kozyrev SV, Leroux L, Durel B, et al. Partial rescue of insulin receptor-deficient mice by transgenic complementation with an activated insulin receptor in the liver. Gene. 2002;299:219–25.
60. Okamoto H, Nakae J, Kitamura T, Park BC, Dragatsis I, Accili D. Transgenic rescue of insulin receptor-deficient mice. J Clin Invest. 2004;114:214–23.
61. Okamoto H, Obici S, Accili D, Rossetti L. Restoration of liver insulin signaling in Insr knockout mice fails to normalize hepatic insulin action. J Clin Invest. 2005;115:1314–22.
62. Girard J, Ferre P, Pegorier JP, Duee PH. Adaptations of glucose and fatty acid metabolism during perinatal period and suckling-weaning transition. Physiol Rev. 1992;72:507–62.
63. Baudry A, Lamothe B, Bucchini D, Jami J, Montarras D, Pinset C, et al. IGF-1 receptor as an alternative receptor for metabolic signaling in insulin receptor-deficient muscle cells. FEBS Lett. 2001;488:174–8.
64. Wang QA, Tao C, Gupta RK, Scherer PE. Tracking adipogenesis during white adipose tissue development, expansion and regeneration. Nat Med. 2013;19:1338–44.
65. Charalambous M, Ferron SR, Da Rocha ST, Murray AJ, Rowland T, Ito M, et al. Imprinted gene dosage is critical for the transition to independent life. Cell Metab. 2012;15:209–21.
66. Riegl SD, Starnes C, Jima DD, Baptissart M, Diehl AM, Belcher SM, et al. The imprinted gene Zac1 regulates steatosis in developmental cadmium-induced nonalcoholic fatty liver disease. Toxicol Sci. 2023;191:34–46.
67. Luo L, Jiang W, Liu H, Bu J, Tang P, Du C, et al. De-silencing Grb10 contributes to acute ER stress-induced steatosis in mouse liver. J Mol Endocrinol. 2018;60:285–97.

68. McNelis K, Yodoshi T, Divanovic S, Gandhi C, Kim JH, Anton CG, et al. Hepatic steatosis in infancy: the beginning of pediatric nonalcoholic fatty liver disease? JPGN Reports. 2021;2:e113.
69. Riazi K, Azhari H, Charette JH, Underwood FE, King JA, Afshar EE, et al. The prevalence and incidence of NAFLD worldwide: a systematic review and meta-analysis. Lancet Gastroenterol Hepatol. 2022;7:851–61.
70. Coan PM, Angiolini E, Sandovici I, Burton GJ, Constância M, Fowden AL. Adaptations in placental nutrient transfer capacity to meet fetal growth demands depend on placental size in mice. J Physiol. 2008;586:4567–76.
71. Kitamura T, Kitamura Y, Nakae J, Giordano A, Cinti S, Kahn CR, et al. Mosaic analysis of insulin receptor function. J Clin Invest. 2004;113:209–19.
72. Ogawa W, Araki E, Ishigaki Y, Hirota Y, Maegawa H, Yamauchi T, et al. New classification and diagnostic criteria for insulin resistance syndrome. Diabetol Int. 2022;13:337–43.
73. Serpente P, Zhang Y, Islimye E, Hart-Johnson S, Gould AP. Quantification of fetal organ sparing in maternal low-protein dietary models. Wellcome Open Res. 2022;6:218.
74. Burns JL, Hassan AB. Cell survival and proliferation are modified by insulin-like growth factor 2 between days 9 and 10 of mouse gestation. Development. 2001;128:3819–30.
75. Stanger BZ, Tanaka AJ, Melton DA. Organ size is limited by the number of embryonic progenitor cells in the pancreas but not the liver. Nature. 2007;445:886–91.

Publisher's Note